

MOL #90951

**Title:** Modeling the effects of  $\beta_1$ -adrenergic receptor blockers and polymorphisms on cardiac myocyte  $\text{Ca}^{2+}$  handling

**Author Names:** Robert K. Amanfu, Jeffrey J. Saucerman

**Author Affiliations (all authors):**

Department of Biomedical Engineering, University of Virginia; Robert M. Berne Cardiovascular Research Center, University of Virginia (R.K.A. and J.J.S.)

MOL #90951

**Running Title:** Modeling  $\beta$ -blockers in cardiac myocytes

**Corresponding Author:**

Jeffrey J. Saucerman, Ph.D.

Department of Biomedical Engineering  
PO Box 800759  
Charlottesville, VA 22908  
United States of America

Email: jsaucerman@virginia.edu  
Phone: (434) 924-5095  
Fax: (434) 982-3870

Pages: 22

Tables: 0

Figures: 7

References: 45

Abstract words: 173

Introduction words: 510

Discussion words: 1025

**Abbreviations:**  $\beta_1$ -AR,  $\beta_1$ -adrenergic receptor; ETCM, extended ternary complex model; FRET, Förster resonance transfer energy transfer; GPP, guanosine 5'-[ $\beta,\gamma$ -imido] triphosphate; IBMX, 3-isobutyl-1-methylxanthine;

MOL #90951

## Abstract

$\beta$ -adrenergic receptor blockers ( $\beta$ -blockers) are commonly used to treat heart failure, but the biological mechanisms governing their efficacy are still poorly understood. The complexity of  $\beta$ -adrenergic signaling coupled with the influence of receptor polymorphisms makes it difficult to intuit the effect of  $\beta$ -blockers on cardiac physiology. While some studies indicate that  $\beta$ -blockers are efficacious by inhibiting  $\beta$ -adrenergic signaling, other studies suggest that they work by maintaining  $\beta$ -adrenergic responsiveness. Here we use a systems pharmacology approach to test the hypothesis that in ventricular myocytes, these two apparently conflicting mechanisms for  $\beta$ -blocker efficacy can occur concurrently. We extended a computational model of the  $\beta_1$ -adrenergic pathway and excitation-contraction coupling to include detailed receptor interactions for 19 ligands. Model predictions, validated with  $\text{Ca}^{2+}$  and FRET imaging of adult rat ventricular myocytes, surprisingly suggest that  $\beta$ -blockers can both inhibit and maintain signaling depending on the magnitude of receptor stimulation. The balance of inhibition and maintenance of  $\beta_1$ -adrenergic signaling is predicted to depend on the specific  $\beta$ -blocker (with greater responsiveness for metoprolol than carvedilol) and  $\beta_1$ -adrenergic receptor Arg389Gly polymorphisms.

MOL #90951

## Introduction

$\beta$ -adrenergic receptor blockers ( $\beta$ -blockers) are front-line therapies for the treatment of heart failure, yet the biological mechanism governing their success is still poorly understood (El-Armouche and Eschenhagen, 2009; Krum, 2003; Tilley and Rockman, 2006). The  $\beta_1$ -adrenergic receptor pathway has a dominant role in the regulation of heart contractility (Saucerman and McCulloch, 2006). One of the hallmarks of heart failure is elevated catecholamine release, which desensitizes the  $\beta$ -adrenergic pathway causing an inability to increase contractility and cardiac output in response to acute stress (Ungerer et al., 1994). Two apparently conflicting theories commonly postulated are that  $\beta$ -blockers are effective in heart failure by either inhibiting the harmful consequences of sustained adrenergic stimulation or maintaining the beneficial aspects of  $\beta_1$ -adrenergic receptor pathway activation (Lohse et al., 2003). The inhibition hypothesis is supported by clinical and experimental evidence that  $\beta$ -blockers help prevent or reverse the cardiac remodeling that leads to heart failure (Lowe et al., 1999). Conversely, the maintenance hypothesis is given credence by clinical evidence that  $\beta$ -blockers increase  $\beta_1$ -adrenergic receptor levels (Michel et al., 1988) and exercise tolerance (Engelmeier et al., 1985).

The ability of different  $\beta$ -blockers to either inhibit or maintain signaling is varied, causing controversy about which  $\beta$ -blocker is more effective in heart failure (Metra et al., 2006). Among the 17 FDA approved  $\beta$ -blockers, a variety of pharmacological properties beyond receptor specificity alone may contribute to these differences (Mason et al., 2009). For example some  $\beta$ -blockers are inverse agonists (Metra et al., 2006), reducing signaling below basal levels (Parra and Bond, 2007). Yet the importance of inverse agonism in determining clinical outcome during  $\beta$ -blocker treatment is unclear.

Genetic differences among patients also impacts  $\beta$ -blocker efficacy (Krum, 2003). *In vitro* experiments in cell expression systems show that the common  $\beta_1$ AR-Arg389Gly single-nucleotide polymorphism has a higher fold increase in adenylyl cyclase activity after receptor stimulation but is more desensitized (Mason et al., 1999; Rathz et al., 2003). Carvedilol and metoprolol have similar affinity for both receptor variants *in vitro* (Joseph et al., 2004), but carvedilol has a larger effect on receptor

MOL #90951

conformation of the  $\beta_1$ -Arg389 variant (Rochais et al., 2007). Thus there may be compound-specific phenotypes for  $\beta_1$ -adrenergic receptor polymorphisms (Dorn and Liggett, 2009).

The complexity of the  $\beta$ -adrenergic receptor pathway coupled with the influence of receptor polymorphisms makes it difficult to intuit the effect of  $\beta$ -blockers on observed cardiac physiology. Here we use a systems pharmacology approach (Sorger and Schoeberl, 2012), extending our previous computational models of  $\beta_1$ -adrenergic signaling and excitation-contraction coupling (Saucerman et al., 2003, 2004) to investigate the apparently conflicting mechanisms by which  $\beta$ -blockers may inhibit or maintain  $\beta$ -adrenergic signaling. We tested the hypothesis that in normal ventricular myocytes, both proposed mechanisms for  $\beta$ -blocker efficacy can occur concurrently. To do this, a previous computational model of the  $\beta_1$ -adrenergic receptor pathway was extended to include detailed receptor interactions for 19 ligands. Model predictions, validated with  $\text{Ca}^{2+}$  and FRET imaging of isolated adult ventricular myocytes, surprisingly suggest that  $\beta$ -blockers can both inhibit and maintain signaling depending on the magnitude of receptor stimulation. In addition, the model predicted  $\beta$ -blocker-specific effects of receptor polymorphisms.

## Materials and Methods

### *Computational model of $\beta$ -blockers and $\beta$ -adrenergic signaling*

A computational model was previously developed that integrates  $\beta_1$ -adrenergic receptor signaling with excitation contraction coupling in rat cardiac myocytes and is based on mass action kinetics (Saucerman et al., 2003). The receptor module was previously described by a ternary complex model (De Lean et al., 1980). To better model the inverse agonism of some  $\beta$ -blockers seen in *in vitro* experiments (Varma et al., 1999), the receptor module of our original  $\beta_1$ -adrenergic receptor signaling model was replaced with the extended ternary complex model (ETCM) (Samama et al., 1993). The ETCM (Figure 1) proposes two receptor states i.e. active and inactive and appropriately describes the constitutive activity of

MOL #90951

$\beta$ -adrenergic receptors. The existence of these receptor states has been recently confirmed by determination of the crystal structure of the  $\beta_2$ -adrenergic receptor (Rosenbaum et al., 2011). Parameters for the ETCM and detailed calibration procedures are described in the Supplemental Methods and Supplemental Table 1. The expanded model has 49 algebraic and differential equations and is constrained by 102 parameters. Sensitivity analysis was used to determine ETCM parameters with distinct effects on model prediction before sequential parameter estimation (Supplemental Figures 1-2). In descriptions comparing model predictions and experimental data, the term calibration or fitting is used to describe instances where model parameters were used to better fit those data, while the term validation is used to describe instances where model parameters were not adjusted to fit those data.

#### *Isolation and culture of rat cardiac myocytes*

All procedures were performed in accordance with the *Guide for the Care and Use of Laboratory Animals* published by the US National Institutes of Health and approved by the University of Virginia Institutional Animal Care and Use Committee. Adult rat ventricular myocytes were isolated similar to Bers et al. (Bers et al., 1990) from adult male (200-250 g) Sprague-Dawley rats. Briefly, rats were anesthetized with ketamine/xylazine and hearts quickly excised before being Langendorff-perfused with collagenase (Cellutron Life Technologies, Baltimore, MD). Ventricular tissue was removed, mechanically dispersed, filtered, and myocyte suspensions rinsed and plated on 35 mm glass coverslips treated with 40  $\mu$ g/ml laminin (Invitrogen, Carlsbad, CA) at a density of  $\sim 3 \times 10^6$  cells per ml. Unattached myocytes were removed after 1 hour by replenishing media. Cells were then loaded with 1  $\mu$ M fluo-4 acetoxymethyl (Gee et al., 2000) (Invitrogen, Carlsbad, CA) or infected with AKAR3 adenovirus (Vector Biolabs, Philadelphia, PA) following manufacturer's instructions in a solution of MEM containing (in mM)  $\text{NaHCO}_3$  4.7, pyruvic acid 2, Na-HEPES 10, HEPES 10 and (in units/ml) insulin 0.4, and penicillin-streptomycin 50 (pH 7.35), Myocytes were then placed in a RC-21BRFS slotted bath chamber (Warner Instruments, Hamden, CT). The chamber was constantly perfused with Tyrodes solution containing (in

MOL #90951

mM) NaCl 140, KCl 4, MgCl<sub>2</sub> 1, and HEPES 10 (pH 7.4) before cells were stimulated with isoproterenol (ISO; Tocris, Minneapolis, MN) and various  $\beta$ -blockers (propranolol, PRO; metoprolol, MET; carvedilol, CAR; Tocris, Minneapolis, MN). The flow rate of the perfusate was approximately 1-1.5 ml/min. Myocytes were field paced with the Myopacer (Ionoptix, Milton, MA) at a frequency of 1 Hz with bipolar pulse duration of 4 ms at a voltage of 10 V. All measurements were performed at room temperature.

#### *Camera-based Ca<sup>2+</sup> imaging of myocytes*

Ca<sup>2+</sup> was measured using fluo-4 as described previously (Amanfu et al., 2011). Myocytes were imaged on an Olympus IX-81 inverted microscope (Olympus, Center Valley, PA) with a Hamamatsu C9300 CCD camera (Bridgewater, NJ) and automated stage (Prior Scientific, Rockland, MA) at a sampling frequency of 67 Hz using Metamorph (Molecular Devices, Sunnyvale, CA). To minimize photobleaching and phototoxicity, cells were imaged intermittently for 10 seconds after every minute. Automated cell segmentation using Otsu's method identified regions of interest from which Ca<sup>2+</sup> transients for each cell were extracted at each time point. Raw fluorescence values were background-subtracted and normalized to yield fold change in fluo-4 intensity:

$$fluo - 4 \text{ fold change} = \frac{\left(\frac{\Delta F}{F_0}\right)_t}{\left(\frac{\Delta F}{F_0}\right)_{t=0}}$$

Average fluo-4 fold change was calculated by averaging 5-7 consecutive transients at specific time points. All segmentation and feature extraction was implemented in MATLAB. Code for these analyses and example movies are freely available at <http://bme.virginia.edu/saucerman>.

#### *FRET imaging of cardiac myocytes*

MOL #90951

Adenovirus was constructed from plasmid DNA of AKAR3 protein kinase-A reporter (Allen and Zhang, 2006). Myocytes were infected with adenovirus immediately following isolation in serum MEM media for 1 hour. Cells were then cultured for 24 hours in serum free MEM media. Myocytes were pre-incubated in solutions of 0.1  $\mu\text{M}$  isoproterenol with and without 0.1  $\mu\text{M}$  propranolol. Cells were placed in a slotted bath with Tyrodes perfusate and paced at 10 Hz. Expressing myocytes were imaged on an Olympus IX-81 inverted microscope with a Hamamatsu C9300 CCD camera. A cocktail of 10  $\mu\text{M}$  forskolin (FSK; Tocris, Minneapolis, MN) and 100  $\mu\text{M}$  3-isobutyl-1-methylxanthine (Sigma-Aldrich, St. Louis, MO) was used as positive control at the end of each experiment. Automated cell segmentation and FRET computation (using PFRET algorithm (Chen and Periasamy, 2006)) were performed in MATLAB. FRET response was normalized to positive control.

## Results

### *Calibration and validation of $\beta_1$ -adrenergic model with extended ternary complex receptor model*

To quantitatively investigate how  $\beta$ -blockers modulate  $\beta$ -adrenergic signaling in cardiac myocytes, a computational model of the  $\beta_1$ -adrenergic receptor pathway was developed that includes detailed interactions between ligand, receptor and G-protein in the form of the extended ternary complex model (Figure 1). The integrated model describes stimulation of the  $\beta_1$ -adrenergic receptor, activation of receptor intermediates, production of cAMP, activation of PKA, phosphorylation of downstream PKA targets and its effect on  $\text{Ca}^{2+}$  transients. Receptor desensitization by both the  $\beta$ -adrenergic receptor kinase and PKA is also included.

Model predictions were compared with a range of experimental data from the literature and the current study (Figure 2). The shift in agonist binding to the receptor in the presence of GPP (which displaces the G protein) was validated (Figure 2A). The model validates reasonably well against measured kinetics of cAMP (Figure 2B) and PKA activity (Figure 2D) in response to isoproterenol. The



MOL #90951

model is calibrated to have appropriate basal and maximally stimulated cAMP levels in cardiac myocytes, with validation of the sensitivity to isoproterenol (Figure 2C). The EC<sub>50</sub> of isoproterenol for phosphorylation of phospholamban by PKA is also accurately validated (Figure 2E). The model was calibrated to have an appropriate EC<sub>50</sub> of isoproterenol for Ca<sup>2+</sup> transients to isoproterenol, as measured with fluo-4 by our group and others (Figure 2F). In addition, we validated model predictions of Ca<sup>2+</sup> transient response to increasing propranolol concentration in the presence of 0.1 μM isoproterenol (Supplemental Figure 4). A summary of all calibrations and validations is provided in Supplemental Table 2. These results indicate that the updated model is consistent with experimental data at multiple levels of the β<sub>1</sub>-adrenergic receptor pathway, providing confidence in the utility of the model for testing hypotheses regarding β-blocker efficacy.

*Propranolol inhibits and maintains the β-adrenergic response depending on the magnitude of receptor stimulation*

While inhibition and maintenance of β-adrenergic responsiveness are typically thought to be incompatible explanations of β-blocker efficacy, we hypothesized that both could occur depending on the magnitude of receptor stimulation. To test this hypothesis *in silico*, we simulated low (0.1 μM) and then high (10 μM) levels of isoproterenol in the absence and presence of the first generation β-blocker propranolol. 0.1 μM propranolol was used because this was the lowest dose that suppressed Ca<sup>2+</sup> transients at 0.1 μM isoproterenol (Supplemental Figure 3). Low and high doses of isoproterenol are analogous to chronically elevated levels of catecholamines in HF and acutely elevated levels in exercise, respectively. In the absence of propranolol, the model predicts that low receptor stimulation increases Ca<sup>2+</sup> amplitude (Figure 3A), with no further sensitivity to subsequent high levels of isoproterenol (Figure 3B). In the presence of propranolol, responsiveness to low receptor stimulation is suppressed but the pathway maintains sensitivity of Ca<sup>2+</sup> transients to high isoproterenol (Figure 3C). Independent experiments imaging Ca<sup>2+</sup> dynamics in isolated adult rat ventricular myocytes qualitatively validated these model predictions (Figure 3D, E, and F). These simulations and experiments indicate that the

MOL #90951

apparently conflicting roles of the  $\beta$ -blocker propranolol to inhibit signaling and maintain responsiveness are in fact compatible.

To experimentally investigate whether these effects persist with chronic receptor stimulation, cells were pre-treated with a low dose of isoproterenol for 24 hours before subsequent stimulation with high isoproterenol (Figure 4). In the absence of propranolol,  $\text{Ca}^{2+}$  transient amplitude in pre-treated cells was not further sensitive to high isoproterenol (Figure 4C), as  $\text{Ca}^{2+}$  transients were already elevated. In contrast, cells pre-treated with propranolol maintained sensitivity to high dose of isoproterenol in the presence of propranolol, similar to model predictions and the acute experiments (Figure 3). Using a FRET reporter for PKA activity, we found that PKA (upstream of  $\text{Ca}^{2+}$  in the  $\beta_1$ -adrenergic pathway) also maintains sensitivity to high isoproterenol in the presence of propranolol (Figure 4B), again validating model predictions (Supplemental Figure 8).

#### *$\beta$ -blockers differ in their ability to inhibit and maintain $\beta$ -adrenergic responsiveness*

To examine whether the dual role of propranolol in inhibiting and maintaining  $\beta$ -adrenergic responsiveness may be generalized to other  $\beta$ -blockers, we extended the model to 17 additional  $\beta$ -adrenergic receptor ligands. Two key ligand specific properties, ligand dissociation constant ( $K_L$  or  $K_A$ ) and inverse agonism ( $\alpha_L$  or  $\alpha_A$ ), were calibrated using data on ligand binding and adenylyl cyclase activity for these 19 ligands in CHO cells overexpressing human  $\beta_1$ -adrenergic receptor (Hoffmann et al., 2004) (Supplemental Figure 2).

We then performed an *in silico* screen of the 19 ligands for effects on  $\beta$ -adrenergic responsiveness (Figure 5). Similar to simulations in Figure 3, low and then high isoproterenol were simulated in the presence and absence of the indicated ligand at 1  $\mu\text{M}$ . The model predicted substantial diversity in the ability of ligands to maintain cAMP sensitivity to subsequent high dose isoproterenol (Figure 5A). To understand this diversity, we examined correlations between cAMP sensitivity and the ligand specific parameters  $K_L$  and  $\alpha$ . As shown in Figure 5B, ligand binding affinity was predicted to influence cAMP sensitivity in a biphasic manner (e.g. metoprolol had the highest cAMP sensitivity with a

MOL #90951

moderate  $K_L$ ). In order for the initial binding event to occur, a  $\beta$ -blocker needs to have a low enough binding affinity to compete out the receptor agonist. There is also a modest positive correlation between  $\alpha$  and cAMP sensitivity, suggesting that ligands with high  $\alpha$  (indicating a high degree of inverse agonism) preferentially increase cAMP sensitivity (Figure 5B). This is due to such ligands keeping the receptor in an inactive state, preventing receptor desensitization (Supplemental Figures 8-10). Neither ligand binding affinity nor inverse agonism is sufficient alone to predict cAMP sensitivity. Thus the ability of  $\beta$ -blockers like metoprolol to maintain cAMP sensitivity was due to both inverse agonism and binding affinity.

#### *Metoprolol and carvedilol differ in their ability to maintain $\beta$ -adrenergic responsiveness*

An interesting prediction of the *in silico* screen is that carvedilol and metoprolol (two clinically prescribed  $\beta$ -blockers) differ significantly in their ability to enhance cAMP sensitivity. This difference indicates that the two drugs may have distinct effects (inhibition or maintenance) on the  $\beta_1$ -adrenergic response. To experimentally validate model predictions for carvedilol and metoprolol,  $Ca^{2+}$  imaging experiments in adult rat ventricular myocytes were performed. As with propranolol, we empirically selected doses for carvedilol and metoprolol that were just sufficient to suppress response to 0.1  $\mu$ M isoproterenol (Supplemental Figure 4). Sensitivity to high isoproterenol was maintained in cardiac myocytes treated with 1  $\mu$ M metoprolol (Figure 6A) but suppressed with 1  $\mu$ M carvedilol (Figure 6B), qualitatively validating our model predictions (summarized in Figure 6C and D),

To test the robustness of this result to  $\beta$ -blocker concentration, we further simulated how cAMP sensitivity is affected by propranolol, metoprolol and carvedilol doses. The model predicted that propranolol and metoprolol robustly maintained  $\beta$ -adrenergic responsiveness, but that at doses lower than we had previously examined, carvedilol may also maintain  $\beta$ -adrenergic responsiveness (Supplemental Figure 5). To test this prediction, we performed subsequent experiments with 0.3  $\mu$ M carvedilol (Supplemental Figure 6), which showed that lower carvedilol still suppressed the responsiveness to high isoproterenol. The robust suppression seen in the carvedilol experiments can be explained by an alternative receptor model accounting for binding of carvedilol to an allosteric site on the  $\beta_1$ -adrenergic

MOL #90951

receptor (Supplemental Figure 7), as supported by previous experiments by Kindermann et al. (Kindermann et al., 2004).

### *Receptor polymorphisms are differentially modulated by diverse $\beta$ -blockers*

Genetic differences among patients also impacts  $\beta$ -blocker efficacy (Shin and Johnson, 2010). Patients with the  $\beta_1$ -Arg389 variant have a better prognosis following  $\beta$ -blocker administration compared with patients with the  $\beta_1$ -Gly389 polymorphism. Increased G protein binding is observed experimentally for the  $\beta_1$ -Arg389 variant causing higher constitutive activity. This behavior was modeled by altering  $K_G$ , the ETCM model parameter that affects binding of active receptor to G-protein.  $K_G$  in the  $\beta_1$ -Arg389 model was manually calibrated to 0.7  $\mu\text{M}$  to replicate the shift in agonist binding in the presence of GPP (Figure 7A) and the higher constitutive activity of the Arg389 variant (Figure 7B).  $\beta_1$ -Arg389 and  $\beta_1$ -Gly389 polymorphisms were predicted to have varying responses to PRO. Propranolol had more of an effect inhibiting the low isoproterenol cAMP and  $\text{Ca}^{2+}$  response in the Arg389 variant (Figure 7C) but also enhanced sensitivity to high isoproterenol. The 19 ligands were predicted to have varying effect on cAMP sensitivity (Figure 7D), similar to the  $\beta_1$ -Gly389 variant (Figure 5A). However, there are some significant differences in the response to particular ligands between the receptor polymorphisms (Figure 7E). For example, atenolol was predicted to be less effective at maintaining  $\beta$ -adrenergic responsiveness for the  $\beta_1$ -Arg389 variant compared with the  $\beta_1$ -Gly389 variant. This diversity of responses indicates that computational models may be useful for predicting pharmacogenetic interactions.

## **Discussion**

### *Mechanisms of $\beta$ -blocker efficacy in heart failure*

A key feature of heart failure (HF) is the modest chronic elevation of circulating catecholamines (e.g. epinephrine) which desensitizes the  $\beta$ -adrenergic receptor signaling pathway, rendering patients

MOL #90951

incapable of increasing cardiac output in response to intense acute stress (e.g. exercise). Crucial alterations to the signaling pathway in this chronically activated state include reduced  $\beta_1$ -adrenergic receptor density (Bristow et al., 1982) and  $\text{Ca}^{2+}$  (Harding et al., 1992) in response to adrenergic stimulation. Sustained stimulation has detrimental long term consequences including apoptosis and hypertrophy (Communal et al., 1998; Taimor et al., 2001). Maintenance of signaling in cardiomyopathy by adenylyl cyclase overexpression (Roth et al., 1999) or G-protein receptor kinase 2 inhibition (Reinkober et al., 2012) has improved cardiac function in *in vitro* murine models. Previous studies of mechanisms governing  $\beta$ -blocker efficacy have focused exclusively on one of two mechanisms i.e. the inhibition (Loves et al., 1999) or maintenance of  $\beta_1$ -adrenergic receptor signaling (Engelmeier et al., 1985; Michel et al., 1988). With evidence supporting both theories, it is unclear how these two contradictory mechanisms can explain the same biological phenomena or the appropriate context where one mechanism dominates. This study provides evidence that at least in normal isolated adult ventricular myocytes, both mechanisms can occur concurrently dependent on the magnitude of receptor stimulation.

Complexities at the receptor level and the influence of receptor polymorphisms complicate attempts to infer these mechanisms. Computational modeling is highly suited for this task by allowing the unbiased comparison of clinically available  $\beta$ -blockers. Previous computational models of the  $\beta_1$ -adrenergic receptor pathway have used simplified receptor kinetic models (Saucerman et al., 2003, 2004). Although sufficient to describe the activation of the signaling pathway by agonists, these pathway models do not have the mechanistic detail of receptor kinetics needed to adequately model the inverse agonism of  $\beta$ -blockers. Detailed receptor models have been developed but these models have been evaluated in isolation from downstream signaling pathways (Samama et al., 1993). To model  $\beta$ -blockers, detailed models of receptor kinetics were linked to the cardiac  $\beta_1$ -adrenergic receptor pathway and excitation contraction coupling. Computational model simulations indicate that both inhibition and maintenance of signaling are compatible, dependent on the magnitude of receptor stimulation. Propranolol inhibited low dose isoproterenol (analogous to chronic levels of catecholamine seen in heart failure) but enabled

MOL #90951

sensitivity to high dose isoproterenol (analogous to acute catecholamine levels during exercise). Fluo-4 and FRET imaging of isolated cardiac myocytes confirmed this prediction.

#### *Metoprolol and carvedilol have distinct mechanisms of action in isolated ventricular myocytes*

Separate clinical trials of the two  $\beta$ -blockers commonly used to treat heart failure show reduction in mortality. Results of the COMET trial, which aimed to compare both treatments, concluded that carvedilol had a larger effect on mortality (Poole-Wilson et al., 2003). Significant controversy surrounds this result with questions raised on the appropriate dose of each compound that merits fair comparison (Kveiborg et al., 2007). Another important clinical measure of heart failure treatment effectiveness is exercise tolerance. Studies have shown that metoprolol has a larger effect on exercise tolerance versus carvedilol (Metra et al., 2000). Our computer simulations and  $\text{Ca}^{2+}$  imaging experiments confirm that metoprolol maintains  $\beta$ -adrenergic signaling in isolated ventricular myocytes due to its moderate binding affinity and high inverse agonism. Carvedilol, although also an inverse agonist, did not maintain isoproterenol sensitivity due to its tight binding to the  $\beta_1$ -adrenergic receptor and potential contribution from allosteric binding (Kindermann et al., 2004).

#### *Pharmacogenomic targeted treatment with $\beta$ -blockers*

Another factor complicating treatment of heart failure patients is the presence of  $\beta$ -adrenergic receptor polymorphisms.  $\beta_1$ -Gly389 has been shown to couple less effectively to G-protein in expression cell systems but the  $\beta_1$ -Arg389 variant provides higher risk to heart failure and differential response to  $\beta$ -blockers. A recent study has shown that carvedilol exhibits enhanced inverse agonism with the  $\beta_1$ -Arg389 variant (Rochais et al., 2007), an example of the potential for personalized medicine. Understanding how genotype affects therapeutic response is expected to open a new era of pharmacogenomics and personalized medicine. One obstacle is that existing knowledge of  $\beta_1$ -adrenergic receptor polymorphisms comes from cell lines and they may function differently in healthy or failing myocytes. We modeled  $\beta_1$ -adrenergic receptor polymorphisms in the background of a ventricular myocyte. The model identified

MOL #90951

differences between the receptor polymorphisms cAMP sensitivity to high isoproterenol in the presence of particular ligands. For example, atenolol was predicted to be less effective at maintaining  $\beta$ -adrenergic responsiveness in isolated ventricular myocytes expressing  $\beta_1$ -Arg389 compared with the  $\beta_1$ -Gly389 variant.

### *Limitations and Considerations*

A critical decision in developing computational models is specifying its scope. Uncertainty in parameters, and henceforth the ensuing predictions, becomes overwhelming as model scope increases. We have restricted our model to the  $\beta_1$ -adrenergic receptor pathway and its effects on  $\text{Ca}^{2+}$  transients in isolated rat ventricular myocytes, because this pathway plays a central role enhancing contractility following  $\beta$ -adrenergic stimulation. However, an alternative hypothesis is that other properties of  $\beta$ -blockers (i.e. binding to other adrenergic receptors and pharmacokinetic properties including half-life, lipid solubility and non-specific binding) may play a larger role than blockade of the  $\beta_1$ -adrenergic receptors. Indeed our simulations suggest that binding of carvedilol to an allosteric site on the  $\beta_1$ -adrenergic receptor influences its effect on  $\beta$ -adrenergic responsiveness. Our current computational model is not yet able to fully explore the consequence of this mechanism *in vivo*. Future work could couple the  $\beta_1$ -adrenergic signaling model to whole-body pharmacokinetics or simulate crosstalk with other adrenergic receptors including the  $\beta_2$ -adrenergic receptor (Zamah et al., 2002).

### *Conclusions*

Previous studies have suggested two seemingly conflicting mechanisms (inhibition or maintenance of the  $\beta$ -adrenergic receptor signaling pathway) to explain  $\beta$ -blocker efficacy. Here we show both in pathway models and adult ventricular myocytes that the  $\beta$ -blockers propranolol and metoprolol (but not carvedilol) not only block response to low isoproterenol (analogous to chronic stimulation in HF) but maintain the  $\beta$ -adrenergic receptor response to subsequent high isoproterenol (analogous to acute stimulation in exercise). Thus both inhibition and maintenance of signaling can occur concurrently

MOL #90951

dependent on the magnitude of receptor stimulation. Computational simulations indicate that these responses are modulated by particular receptor polymorphisms. Evaluating the mechanisms for these differences, with the help of computational models, is an important step towards designing personalized  $\beta$ -blocker therapies.

### **Acknowledgements**

The authors thank Renata Polanowska-Grabowska for technical assistance.

### **Authorship Contributions**

*Participated in research design:* Amanfu and Saucerman

*Conducted experiments:* Amanfu

*Contributed new reagents or analytic tools:* Amanfu

*Performed data analysis:* Amanfu

*Wrote or contributed to the writing of the manuscript:* Amanfu and Saucerman



MOL #90951

## References

- Allen, M.D., and Zhang, J. (2006). Subcellular dynamics of protein kinase A activity visualized by FRET-based reporters. *Biochem. Biophys. Res. Commun.* 348, 716–721.
- Amanfu, R.K., Muller, J.B., and Saucerman, J.J. (2011). Automated image analysis of cardiac myocyte Ca<sup>2+</sup> dynamics. In 2011 Annual International Conference of the IEEE Engineering in Medicine and Biology Society, EMBC, (IEEE), pp. 4661–4664.
- De Arcangelis, V., Liu, S., Zhang, D., Soto, D., and Xiang, Y.K. (2010). Equilibrium between Adenylyl Cyclase and Phosphodiesterase Patterns Adrenergic Agonist Dose-Dependent Spatiotemporal cAMP/Protein Kinase A Activities in Cardiomyocytes. *Mol. Pharmacol.* 78, 340–349.
- Bers, D.M., Lederer, W.J., and Berlin, J.R. (1990). Intracellular Ca transients in rat cardiac myocytes: role of Na-Ca exchange in excitation-contraction coupling. *Am. J. Physiol. - Cell Physiol.* 258, C944–C954.
- Bristow, M., Ginsburg, R., Minobe, W., Cubicciotti, R., Sageman, W., Lurie, K., Billingham, M., Harrison, D., and Stinson, E. (1982). Decreased catecholamine sensitivity and  $\beta$ -adrenergic receptor density in failing human hearts. *N Engl J Med* 307, 205–211.
- Chen, Y., and Periasamy, A. (2006). Intensity Range Based Quantitative FRET Data Analysis to Localize Protein Molecules in Live Cell Nuclei. *J. Fluoresc.* 16, 95–104.
- Collins, H.E., and Rodrigo, G.C. (2010). Inotropic Response of Cardiac Ventricular Myocytes to - Adrenergic Stimulation With Isoproterenol Exhibits Diurnal Variation. Involvement of Nitric Oxide. *Circ. Res.*
- Communal, C., Singh, K., Pimentel, D.R., and Colucci, W.S. (1998). Norepinephrine Stimulates Apoptosis in Adult Rat Ventricular Myocytes by Activation of the  $\beta$ -Adrenergic Pathway. *Circulation* 98, 1329–1334.
- Dorn, G.W., and Liggett, S.B. (2009). Mechanisms of Pharmacogenomic Effects of Genetic Variation within the Cardiac Adrenergic Network in Heart Failure. *Mol. Pharmacol.* 76, 466–480.
- El-Armouche, A., and Eschenhagen, T. (2009).  $\beta$ -Adrenergic stimulation and myocardial function in the failing heart. *Heart Fail. Rev.*
- Engelmeier, R.S., O'Connell, J.B., Walsh, R., Rad, N., Scanlon, P.J., and Gunnar, R.M. (1985). Improvement in symptoms and exercise tolerance by metoprolol in patients with dilated cardiomyopathy: a double-blind, randomized, placebo-controlled trial. *Circulation* 72, 536–546.
- Gee, K.R., Brown, K.A., Chen, W.-N.U., Bishop-Stewart, J., Gray, D., and Johnson, I. (2000). Chemical and physiological characterization of fluo-4 Ca<sup>2+</sup>-indicator dyes. *Cell Calcium* 27, 97–106.
- Harding, S.E., Jones, S.M., O'Gara, P., del Monte, F., Vescovo, G., and Poole-Wilson, P.A. (1992). Isolated ventricular myocytes from failing and non-failing human heart; the relation of age and clinical status of patients to isoproterenol response. *J. Mol. Cell. Cardiol.* 24, 549–564.
- Hoffmann, C., Leitz, M.R., Oberdorf-Maass, S., Lohse, M.J., and Klotz, K.-N. (2004). Comparative pharmacology of human beta-adrenergic receptor subtypes--characterization of stably transfected receptors in CHO cells. *Naunyn. Schmiedebergs Arch. Pharmacol.* 369, 151–159.

MOL #90951

Joseph, S.S., Lynham, J.A., Grace, A.A., Colledge, W.H., and Kaumann, A.J. (2004). Markedly reduced effects of (-)-isoprenaline but not of (-)-CGP12177 and unchanged affinity of  $\beta$ -blockers at Gly389- $\beta$ 1-adrenoceptors compared to Arg389- $\beta$ 1-adrenoceptors. *Br. J. Pharmacol.* 142, 51–56.

Kindermann, M., Maack, C., Schaller, S., Finkler, N., Schmidt, K.I., Laer, S., Wuttke, H., Schafers, H.-J., and Bohm, M. (2004). Carvedilol but not metoprolol reduces beta-adrenergic responsiveness after complete elimination from plasma in vivo. *Circulation* 109, 3182–3190.

Krum, H. (2003). Beta-blockers in chronic heart failure: what have we learned? What do we still need to know? *Curr. Opin. Pharmacol.* 3, 168–174.

Kveiborg, B., Major-Petersen, A., Christiansen, B., and Torp-Pedersen, C. (2007). Carvedilol in the treatment of chronic heart failure: Lessons from The Carvedilol Or Metoprolol European Trial. *Vasc. Health Risk Manag.* 3, 31–37.

De Lean, A., Stadel, J.M., and Lefkowitz, R.J. (1980). A ternary complex model explains the agonist-specific binding properties of the adenylate cyclase-coupled beta-adrenergic receptor. *J. Biol. Chem.* 255, 7108–7117.

Lohse, M.J., Engelhardt, S., and Eschenhagen, T. (2003). What Is the Role of  $\beta$ -Adrenergic Signaling in Heart Failure? *Circ Res* 93, 896–906.

Lowes, B.D., Gill, E.A., Abraham, W.T., Larrain, J.R., Robertson, A.D., Bristow, M.R., and Gilbert, E.M. (1999). Effects of carvedilol on left ventricular mass, chamber geometry, and mitral regurgitation in chronic heart failure. *Am. J. Cardiol.* 83, 1201–1205.

Mason, D.A., Moore, J.D., Green, S.A., and Liggett, S.B. (1999). A Gain-of-function Polymorphism in a G-protein Coupling Domain of the Human  $\beta$ 1-Adrenergic Receptor. *J. Biol. Chem.* 274, 12670–12674.

Mason, R.P., Giles, T.D., and Sowers, J.R. (2009). Evolving Mechanisms of Action of Beta Blockers: Focus on Nebivolol. *J. Cardiovasc. Pharmacol.* 54, 123–128.

Metra, M., Giubbini, R., Nodari, S., Boldi, E., Modena, M.G., and Cas, L.D. (2000). Differential Effects of  $\beta$ -Blockers in Patients With Heart Failure: A Prospective, Randomized, Double-Blind Comparison of the Long-Term Effects of Metoprolol Versus Carvedilol. *Circulation* 102, 546–551.

Metra, M., Cas, L.D., and Cleland, J.G.F. (2006). Pharmacokinetic and Pharmacodynamic Characteristics of [beta]-Blockers: When Differences May Matter. *J. Card. Fail.* 12, 177–181.

Mialet Perez, J., Rathz, D.A., Petrashevskaya, N.N., Hahn, H.S., Wagoner, L.E., Schwartz, A., Dorn, G.W., and Liggett, S.B. (2003). Beta 1-adrenergic receptor polymorphisms confer differential function and predisposition to heart failure. *Nat. Med.* 9, 1300–1305.

Michel, M.C., Pingsmann, A., Beckeringh, J.J., Zerkowski, H.R., Doetsch, N., and Brodde, O.E. (1988). Selective regulation of beta 1- and beta 2-adrenoceptors in the human heart by chronic beta-adrenoceptor antagonist treatment. *Br. J. Pharmacol.* 94, 685–692.

Parra, S., and Bond, R.A. (2007). Inverse agonism: from curiosity to accepted dogma, but is it clinically relevant? *Curr. Opin. Pharmacol.* 7, 146–150.

MOL #90951

- Poole-Wilson, P.A., Swedberg, K., Cleland, J.G., Di Lenarda, A., Hanrath, P., Komajda, M., Lubsen, J., Lutiger, B., Metra, M., Remme, W.J., et al. (2003). Comparison of carvedilol and metoprolol on clinical outcomes in patients with chronic heart failure in the Carvedilol Or Metoprolol European Trial (COMET): randomised controlled trial. *The Lancet* 362, 7–13.
- Rathz, D.A., Gregory, K.N., Fang, Y., Brown, K.M., and Liggett, S.B. (2003). Hierarchy of Polymorphic Variation and Desensitization Permutations Relative to B1- and B2-Adrenergic Receptor Signaling. *J. Biol. Chem.* 278, 10784–10789.
- Reinkober, J., Tscheschner, H., Pleger, S.T., Most, P., Katus, H.A., Koch, W.J., and Raake, P.W.J. (2012). Targeting GRK2 by gene therapy for heart failure: benefits above  $\beta$ -blockade. *Gene Ther.* 19, 686–693.
- Rochais, F., Vilardaga, J.-P., Nikolaev, V.O., Bünemann, M., Lohse, M.J., and Engelhardt, S. (2007). Real-time optical recording of  $\beta$ 1-adrenergic receptor activation reveals supersensitivity of the Arg389 variant to carvedilol. *J. Clin. Invest.* 117, 229–235.
- Rosenbaum, D.M., Zhang, C., Lyons, J.A., Holl, R., Aragao, D., Arlow, D.H., Rasmussen, S.G.F., Choi, H.-J., DeVree, B.T., Sunahara, R.K., et al. (2011). Structure and function of an irreversible agonist- $\beta$ 2 adrenoceptor complex. *Nature* 469, 236–240.
- Roth, D.M., Gao, M.H., Lai, N.C., Drumm, J., Dalton, N., Zhou, J.Y., Zhu, J., Entrikin, D., and Hammond, H.K. (1999). Cardiac-Directed Adenylyl Cyclase Expression Improves Heart Function in Murine Cardiomyopathy. *Circulation* 99, 3099–3102.
- Samama, P., Cotecchia, S., Costa, T., and Lefkowitz, R.J. (1993). A mutation-induced activated state of the  $\beta$ 2-adrenergic receptor. Extending the ternary complex model. *J. Biol. Chem.* 268, 4625–4636.
- Saucerman, J.J., and McCulloch, A.D. (2006). Cardiac  $\beta$ -Adrenergic Signaling: From Subcellular Microdomains to Heart Failure. *Ann. N. Y. Acad. Sci.* 1080, 348–361.
- Saucerman, J.J., Brunton, L.L., Michailova, A.P., and McCulloch, A.D. (2003). Modeling  $\beta$ -Adrenergic Control of Cardiac Myocyte Contractility in Silico. *J. Biol. Chem.* 278, 47997–48003.
- Saucerman, J.J., Healy, S.N., Belik, M.E., Puglisi, J.L., and McCulloch, A.D. (2004). Proarrhythmic consequences of a KCNQ1 AKAP-binding domain mutation: computational models of whole cells and heterogeneous tissue. *Circ. Res.* 95, 1216–1224.
- Shin, J., and Johnson, J.  $\beta$ -Blocker pharmacogenetics in heart failure. *Heart Fail. Rev.*
- Sorger, P.K., and Schoeberl, B. (2012). An expanding role for cell biologists in drug discovery and pharmacology. *Mol. Biol. Cell* 23, 4162–4164.
- Taimor, G., Schlüter, K.-D., and Piper, H.M. (2001). Hypertrophy-associated Gene Induction after  $\beta$ -Adrenergic Stimulation in Adult Cardiomyocytes. *J. Mol. Cell. Cardiol.* 33, 503–511.
- Tilley, D.G., and Rockman, H.A. (2006). Role of beta-adrenergic receptor signaling and desensitization in heart failure: new concepts and prospects for treatment. *Expert Rev. Cardiovasc. Ther.* 4, 417–432.

MOL #90951

Ungerer, M., Parruti, G., Bohm, M., Puzicha, M., DeBlasi, A., Erdmann, E., and Lohse, M. (1994). Expression of beta-arrestins and beta-adrenergic receptor kinases in the failing human heart. *Circ Res* 74, 206–213.

Varma, D.R., Shen, H., Deng, X.F., Peri, K.G., Chemtob, S., and Mulay, S. (1999). Inverse agonist activities of  $\beta$ -adrenoceptor antagonists in rat myocardium. *Br. J. Pharmacol.* 127, 895–902.

Zamah, A.M., Delahunty, M., Luttrell, L.M., and Lefkowitz, R.J. (2002). PKA-mediated phosphorylation of the Beta 2-adrenergic receptor regulates its coupling to Gs and Gi: Demonstration in a reconstituted system. *J. Biol. Chem.* 277, 31249–31256.

MOL #90951

## Footnotes

This work was supported by the American Heart Association [Grant 0830470N] and the National Institutes of Health National Heart Lung and Blood Institute [Grant HL094476 and HL05242].

## Figure Legends

**Figure 1: Extended ternary complex model of the  $\beta_1$ -adrenergic receptor, coupled with the  $\beta_1$ -adrenergic pathway and ventricular myocyte EC coupling.**  $K_L$ , equilibrium dissociation constant of the agonist receptor complex;  $K_R$ , propensity for switching between active and inactive receptor states;  $K_G$ , dissociation constant for binding of G-protein to the receptor;  $\alpha$ , differential affinity of the ligand for the inactive receptor;  $\gamma$ , differential affinity of the ligand-receptor complex for G-protein.

**Figure 2: Experimental validation of coupled  $\beta_1$ -adrenergic signaling and EC coupling model.** **A**, Model reproduces shift in agonist binding affinity in the presence of GPP, which displaces  $G_s$  from the receptor. **B**, Kinetics of [cAMP] in response to 10 nM isoproterenol (ISO) stimulation. **C**, cAMP dose response to ISO. **D**, PKA activity measured by FRET reporter AKAR3. **E**, Phospholamban phosphorylation in response to ISO. **F**,  $Ca^{2+}$  dose response to ISO. Results in A-C, E, F show direct comparison with published experimental data (Mason et al., 1999), (Vila Petroff et al., 2001), (De Arcangelis et al., 2010), (Vittone et al., 1998) and (Collins and Rodrigo, 2010) whereas data in D & F was acquired in the current study.

**Figure 3: Propranolol both inhibits and maintains  $\beta_1$ -adrenergic-mediated regulation of  $Ca^{2+}$  transients.** **A**, Model-predicted individual  $Ca^{2+}$  transients in response to increasing [ISO]. **B**,  $Ca^{2+}$  concentration increased in response to 0.1  $\mu M$  ISO, with no further response to subsequent stimulation with 10  $\mu M$  ISO. **C**, The model predicted that propranolol (PRO) inhibits response to 0.1  $\mu M$  ISO, but the responsiveness to 10  $\mu M$  ISO is maintained (large sensitivity). **D**, Individual  $Ca^{2+}$  transients as measured by fluo-4 from rat ventricular myocytes exposed to increasing [ISO]; scale bar 20  $\mu M$ . **E** Similar to model predictions, myocytes were not responsive to further stimulation with 10  $\mu M$  ISO. **F**, PRO inhibited response to 0.1  $\mu M$  ISO, but myocytes were responsive to further stimulation with 10  $\mu M$  ISO. Sensitivity was quantified as the increase in  $Ca^{2+}$  transient magnitude when increasing from 0.1  $\mu M$  ISO (analogous to chronically elevated catecholamines in heart failure) to 10  $\mu M$  ISO (analogous to exercise).

**Figure 4: Propranolol both inhibits and maintains the  $\beta_1$ -adrenergic-mediated  $Ca^{2+}$  and PKA response following 24 hour ISO pre-treatment.** **A**, Expression and cytosolic distribution of PKA activity biosensor AKAR3 in rat adult ventricular myocytes (YFP emission); scale bar 40  $\mu M$ . Following 24 hour pre-treatment with both 0.1  $\mu M$  ISO and 0.1  $\mu M$  PRO, both **B**) PKA activity measured by AKAR3 and **C**)  $Ca^{2+}$  response as measured by fluo-4 was still sensitive to subsequent increase to 10  $\mu M$  ISO.

**Figure 5: Ligand binding affinity and inverse agonism both predicted to influence ligand cAMP sensitivity.** **A**, In-silico screen of 19  $\beta_1$ -adrenergic ligands predicts differential cAMP sensitivity. **B**, Effect of ligand dissociation constant ( $K_L$ ) on predicted cAMP sensitivity. **C**, Effect of ligand inverse agonism ( $\alpha$ ) on predicted cAMP sensitivity. PRO, metoprolol and carvedilol (highlighted in red) were predicted to have both distinct effects on cAMP sensitivity with distinct combinations of ligand dissociation constant and inverse agonism.

MOL #90951

**Figure 6: Metoprolol and carvedilol differentially influence  $\beta_1$ -adrenergic responsiveness.** **A**, In adult ventricular myocytes, metoprolol (MET) blocked response to 0.1  $\mu$ M ISO, but the responsiveness to 10  $\mu$ M ISO was maintained. **B**, Carvedilol (CAR) blocked the response to both 0.1  $\mu$ M ISO and 10  $\mu$ M ISO. **C**, Summary of model-predicted  $\text{Ca}^{2+}$  response to 0.1  $\mu$ M and 10  $\mu$ M ISO in the presence of  $\beta$ -blockers. MET and PRO were both predicted to substantially enhance cAMP sensitivity to 10  $\mu$ M ISO, but CAR was not. **D**, Summary of experimental validations from adult ventricular myocytes for PRO, MET and CAR.

**Figure 7:  $\beta_1$ AR-Arg389 polymorphism responds differently to  $\beta$ -blockers.** **A**, Model reproduces shift in agonist binding affinity in the presence of GPP for Arg389. **B**, Concentration dependence of adenylyl cyclase (AC) activity to isoproterenol for Gly389 and Arg389. **C**, Arg389 is predicted to have higher cAMP sensitivity and  $\text{Ca}^{2+}$  response versus Gly 389 in cardiac myocytes. **D**, In-silico screen of 19  $\beta_1$ -adrenergic ligands against Arg389. **E**, Differential cAMP sensitivity between Arg389 and Gly389 for different  $\beta_1$ -adrenergic ligands predicted for cardiac myocytes. Experimental data in panels A and B from (Mason et al., 1999; Mialet Perez et al., 2003).

# Figure 1

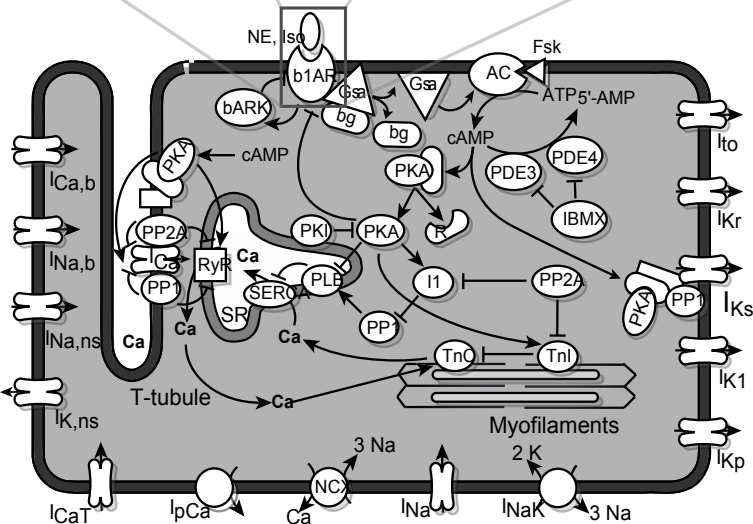
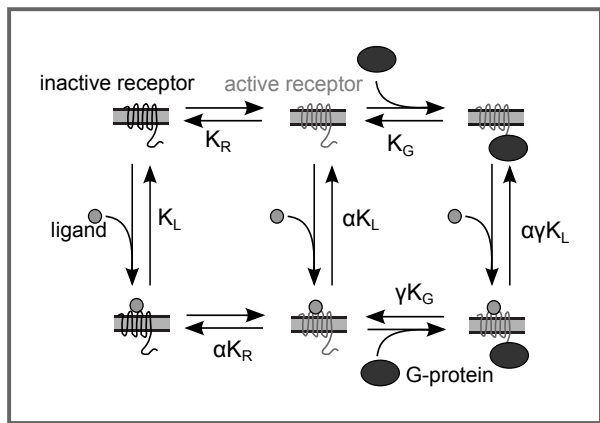
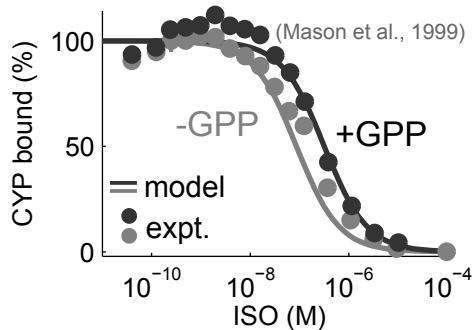
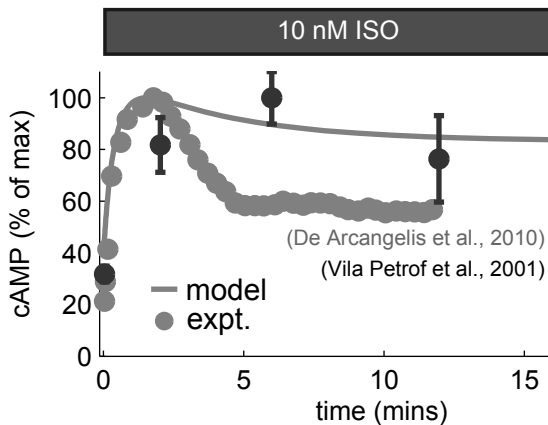


Figure 2

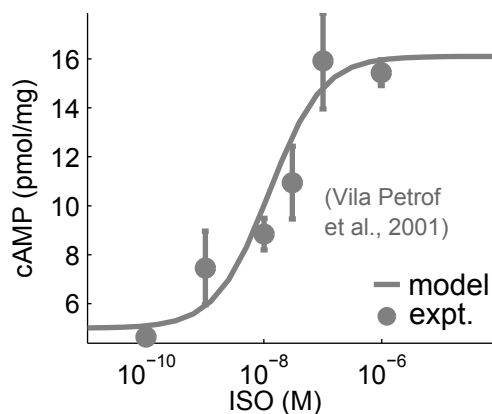
A



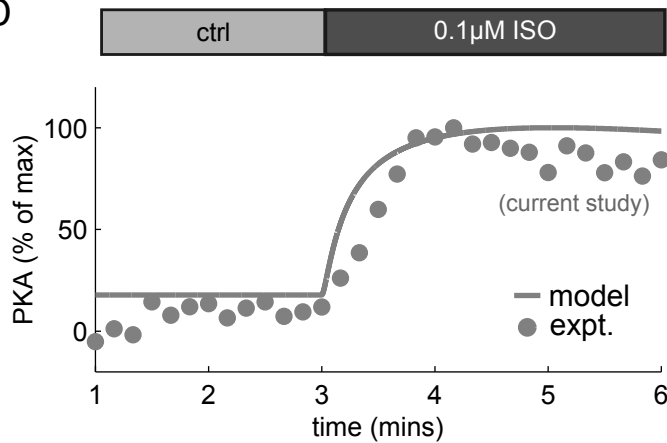
B



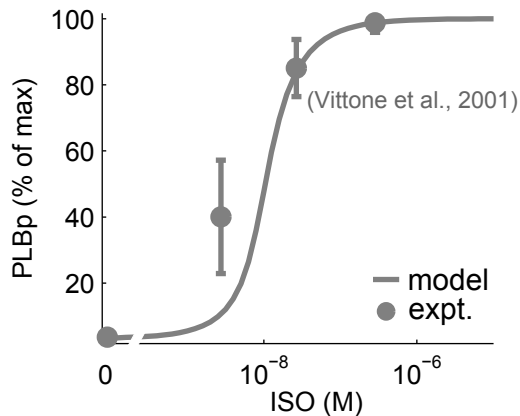
C



D



E



F

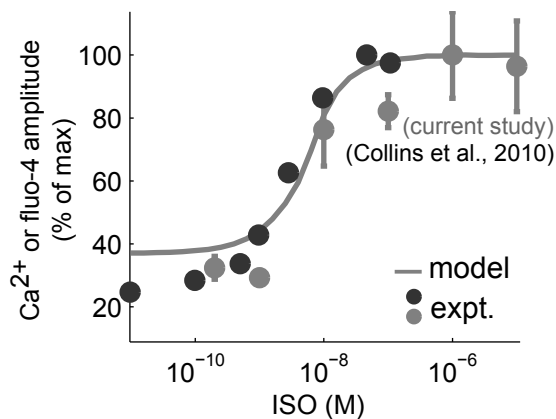


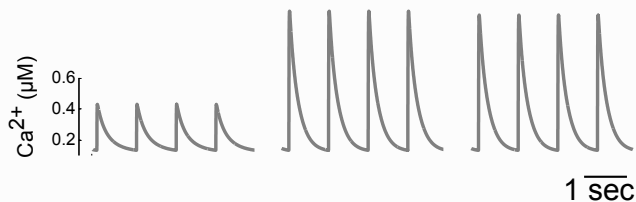


Figure 3

A

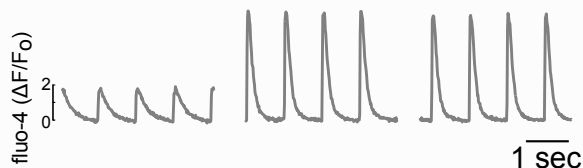


model

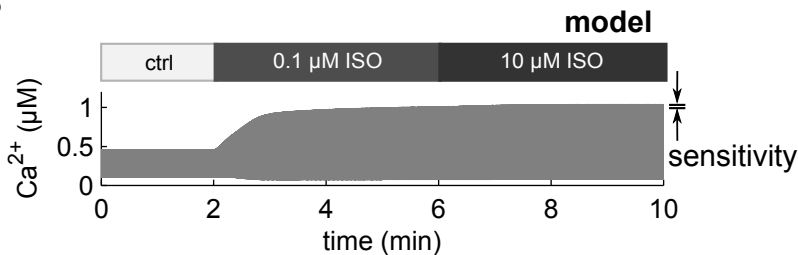
ctrl    0.1  $\mu\text{M}$  ISO    10  $\mu\text{M}$  ISO

D

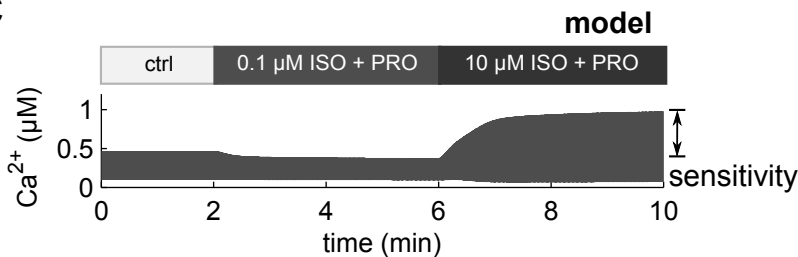
experiment

ctrl    0.1  $\mu\text{M}$  ISO    10  $\mu\text{M}$  ISO

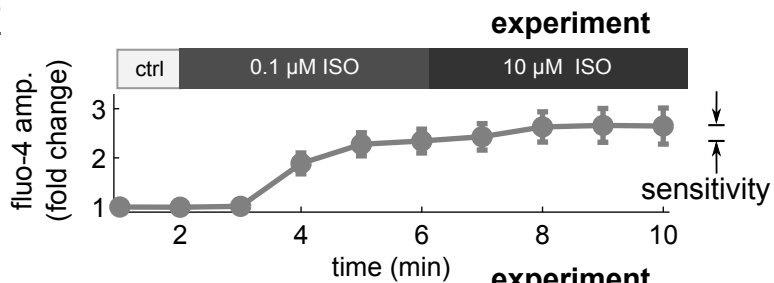
B



C



E



F

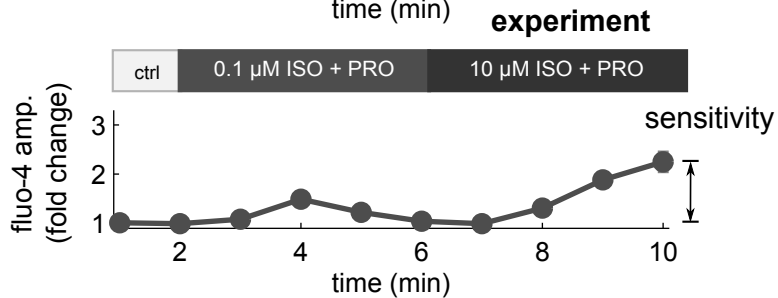
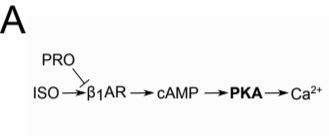
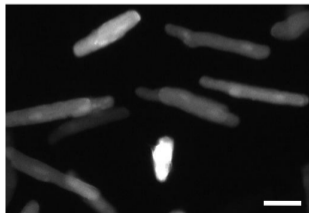


# Figure 4



AKAR3 PKA activity reporter



535/30 emission

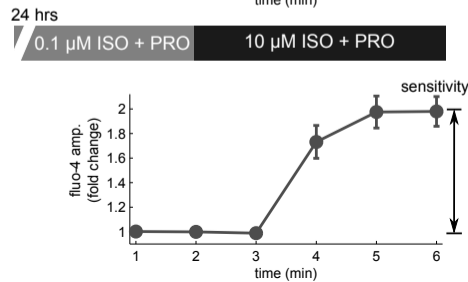
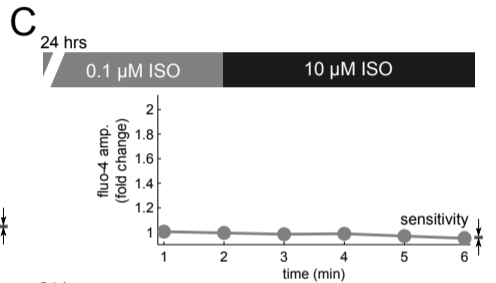
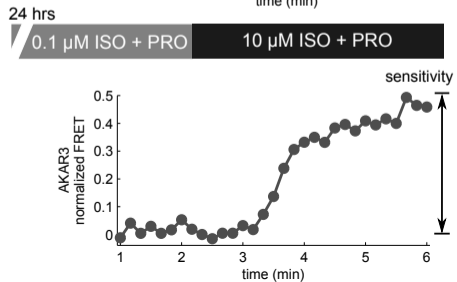
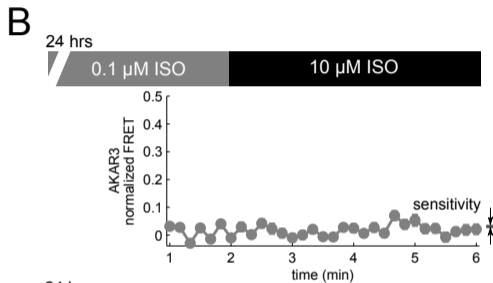
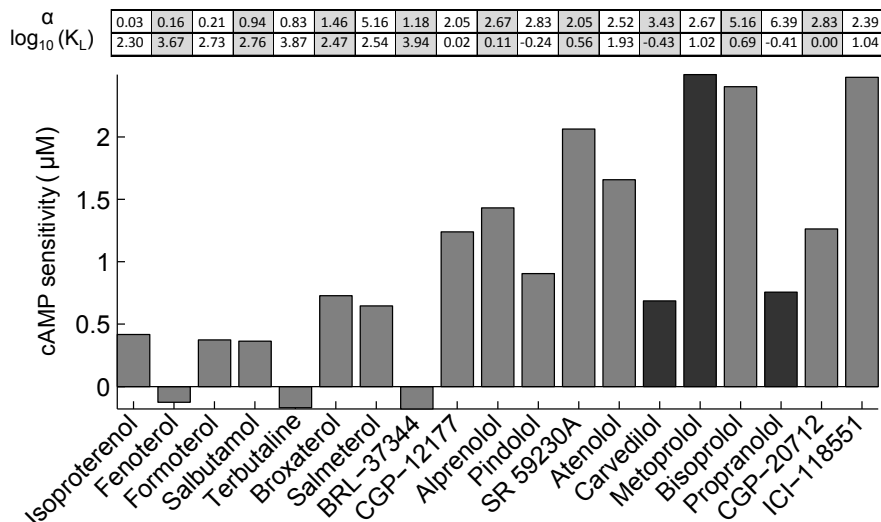
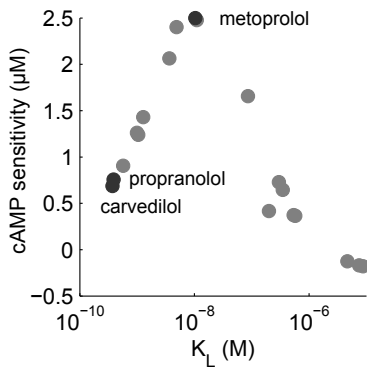


# Figure 5

**A**



**B**



**C**

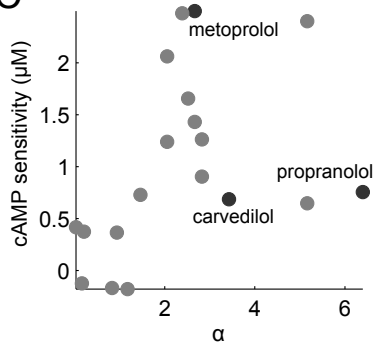
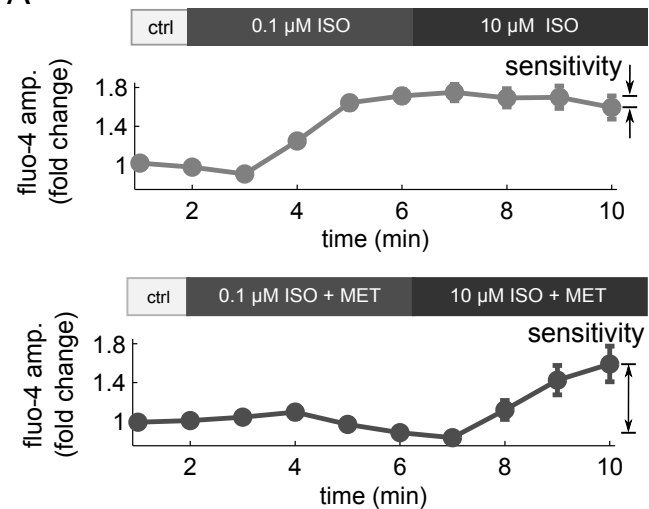
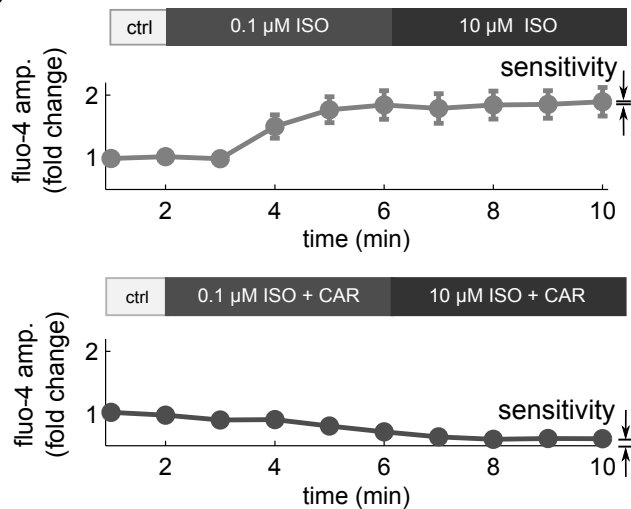


Figure 6

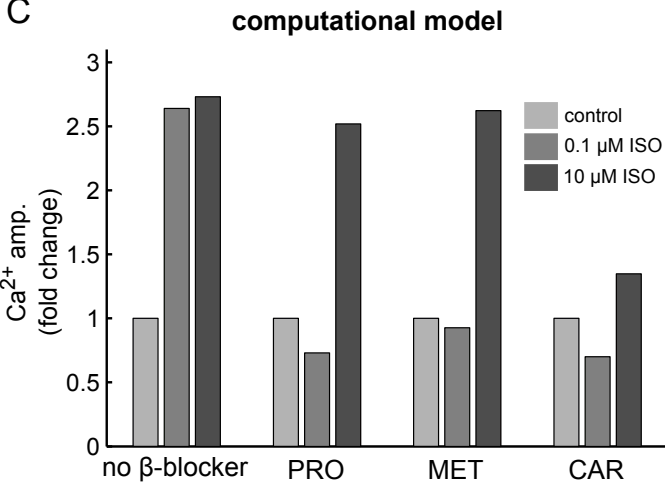
A



B



C



D

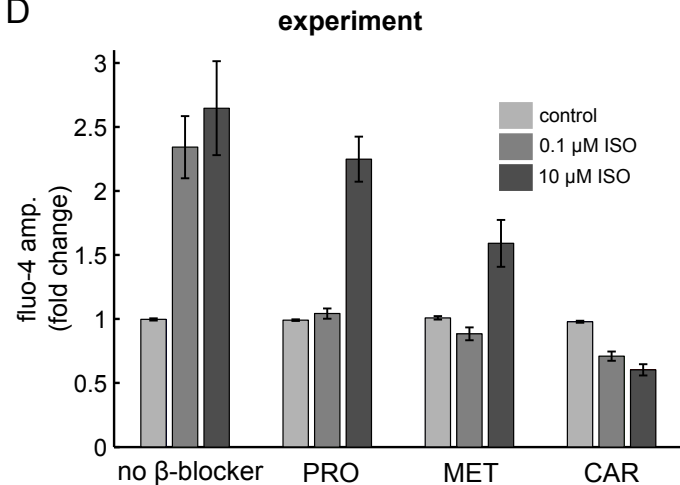
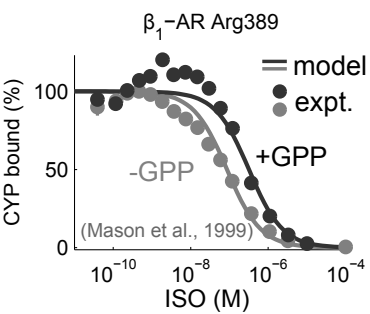
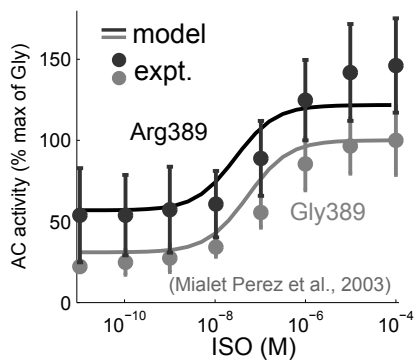


Figure 7

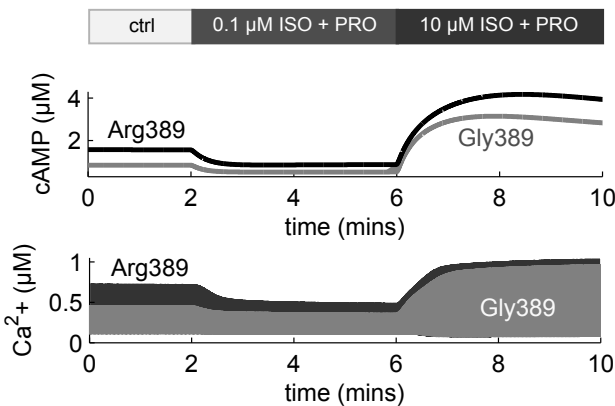
A



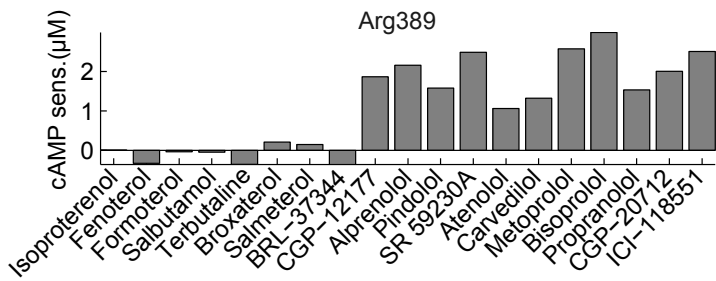
B



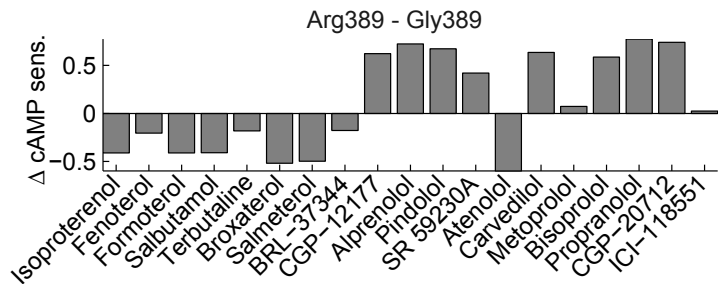
C



D



E



## Supplement for: Molecular Pharmacology

**Title:** Modeling the effects of  $\beta_1$ -adrenergic receptor blockers and polymorphisms on cardiac myocyte  $\text{Ca}^{2+}$  handling

**Author Names:** Robert K. Amanfu, Jeffrey J. Saucerman

### Supplemental Methods

#### *Numerical methods*

The system of differential-algebraic equations was solved in MATLAB (Mathworks, Natick, MA) with the ode15s algorithm. In instances where mass balance of the receptor was violated due to numerical errors, those particular time steps and corresponding state variable values were removed (less than 0.1% of all time steps).

Model calibration was performed with a hybrid nonlinear least squares regression approach, using a genetic algorithm (MATLAB Global Optimization Toolbox function `ga`) followed by a trust-region method (MATLAB Optimization Toolbox function `lsqnonlin`). This hybrid combines the advantages of avoiding local minima (with the genetic algorithm) while efficiently converging in the vicinity of a minimum (with the trust-region method). Optimization parameters used for the genetic algorithm were: initial population of 20 individuals with an initial range of [0; 1], elite children of 2, crossover fraction of 0.8 with function tolerance of  $1 \times 10^{-6}$ . For the trust-region method, maximum iterations were set to 400 with a function tolerance of  $1 \times 10^{-6}$ . The error function minimized in both algorithms was:

$$error = \sum_{i=1}^n (cAMP_{i[model]} - cAMP_{i[experiment]})^2$$

To reduce computational requirements, all model calibration procedures were performed on the signaling pathway model without inclusion of excitation contraction coupling. This is justified because there is no feedback from excitation-contraction coupling to cAMP in our model. Confidence intervals for fitted parameters were estimated using the Cramer-Rao inequality<sup>8</sup>.

#### *Parameter estimation strategy*

As described in detail below, 5 parameters in the extended ternary complex model (ETCM) ( $\beta_1AR_{tot}$ ,  $G_{stot}$ ,  $K_R$ ,  $\gamma_L$ ,  $\gamma_A$ ) were set directly based on model assumptions or previous studies, while 4 parameters

( $K_L$ ,  $K_G$ ,  $\alpha_L$ ,  $\alpha_A$ ) were estimated numerically by calibrating the model to experimental data. In order to constrain parameter values as much as possible, we performed a sensitivity analysis which guided a sequential parameter estimation procedure:

1. ETCM parameters were set equal to values used previously by Samama et al.<sup>4</sup> or Saucerman et al.<sup>1,2</sup> Sensitivity analysis of this initial model revealed the impact of each parameter on downstream cAMP (Supplemental Figure 1). For example  $K_R$  and  $K_G$  predominantly affect basal cAMP while  $\gamma_L$  has a larger effect on maximum cAMP.  $K_L$  specifically affected the  $EC_{50}$ .
2. Several ETCM parameters were held fixed.  $K_R$  was left unaltered from Samama et al.<sup>4</sup> because it is an intrinsic receptor property.  $\gamma_A$  was set to 1, assuming that a  $\beta$ -blocker does not affect the affinity of the active receptor for G-protein.  $\beta 1AR_{tot}$  and  $G_{tot}$  were left unaltered from Saucerman et al. because these had been directly measured in ventricular myocytes. Dissociation constant for G-protein binding to adenylyl cyclase ( $K_{dAC:Gs}$ ) was manually decreased by 50% (from 0.45 in Saucerman et al. to 0.23  $\mu M$ ) to allow sufficient maximum cAMP after switching from TCM to ETCM receptor modules.
3.  $K_G$  (dissociation constant governing G protein binding to the active receptor) was numerically fit to achieve appropriate basal cAMP synthesis rates (0.8400 vs. 0.8400  $\mu M$  cAMP per 20 minutes as measured with *in vitro* cardiac cell membrane assays performed by Vila Petroff et al.<sup>9</sup>).  $K_G$  was determined to be  $2.413 \pm (2.587 \times 10^{-14}) \mu M$ .
4.  $\gamma_L$  was numerically fit to achieve maximum cAMP synthesis rates when stimulated by high dose isoproterenol (ISO) (2.703 vs. 2.703  $\mu M$  cAMP per 20 minutes as measured with *in vitro* cardiac cell membrane assays performed by Vila Petroff et al.<sup>9</sup>).  $\gamma_L$  was determined to be  $0.3762 \pm (3.150 \times 10^{-6})$ .
5.  $\alpha$  (the differential affinity of a ligand for the active receptor) was determined by numerically fitting to cAMP synthesis rates measured by Hoffmann et al.<sup>10</sup> for 19  $\beta$ -adrenergic ligands in CHO cell membrane assays. The influence of ligand binding affinity ( $K_L$ ) was minimized by using saturating concentrations of ligand, as done in Hoffmann et al.<sup>10</sup> To allow relative comparison of cAMP synthesis rates between model and experiment for the 19 ligands, experimental rates from Hoffmann et al. were normalized linearly based on basal (0%) and maximal (100%) cAMP synthesis rates in the model (Supplemental Figure 2A). Consistent with the experimental conditions, simulations were run with PDE inhibition for 20 minutes. Comparisons between model fits and experimental data<sup>10</sup> for the 19 ligands are shown in Supplemental Figure 2B, along with the corresponding estimated  $\alpha$  parameters.

6.  $K_L$  (dissociation constant of agonist) or  $K_A$  (dissociation constant of antagonist) was calculated from binding affinity data in the Hoffmann et al. data set ( $K_i$ ) using the following relationship:

$$K_L \text{ or } K_A = \frac{K_i(\alpha K_R + 1)}{\alpha(K_R + 1)}$$

This equation corrects the measured  $K_i$  to account for spontaneous receptor activity in the ETCM model. When simulating experiments in cardiac myocytes,  $K_L$  for all ligands was further scaled by 0.24 to fit the  $EC_{50}$  of the ISO-calcium dose response in cardiac myocytes (Figure 2F).  $K_L/K_A$  values are shown in Supplemental Figure 2B.

### ***Model Equations and Parameters***

Equations and parameters for the receptor module and related equations are shown below. All other equations and parameters for downstream signaling and excitation-contraction coupling are the same as described previously by Saucerman et al.<sup>1-2</sup>

<b>Parameter</b>	<b>Description</b>	<b>Value</b>	<b>Units</b>	<b>Source</b>
Ltot	agonist concentration (when used)	variable	$\mu\text{M}$	
$\beta_1\text{AR}_{\text{tot}}$	total $\beta_1$ -adrenergic receptors	0.0132	$\mu\text{M}$	Step 2 <sup>1</sup>
Gstot	total Gs protein	3.83	$\mu\text{M}$	Step 2 <sup>1</sup>
$K_R$	propensity for switching between active and inactive receptor states	10		Step 2 <sup>4</sup>
$K_L$	equilibrium dissociation constant of the agonist receptor complex	Supp. Fig 2B	$\mu\text{M}$	Step 6
$K_A$	equilibrium dissociation constant of the antagonist receptor complex	Supp. Fig 2B	$\mu\text{M}$	Step 6
$K_G$	ligand bound $\beta_1$ -AR associating with G-protein	2.413	$\mu\text{M}$	Step 3
$\alpha_L$	differential affinity of the agonist for the inactive receptor	Supp. Fig 2B		Step 5
$\alpha_A$	differential affinity of the antagonist for the inactive receptor	Supp. Fig 2B		Step 5
$\gamma_L$	differential affinity of the agonist-receptor complex for G-protein	0.3762		Step 4
$\gamma_A$	differential affinity of the antagonist-receptor complex for G-protein	1		Step 2
$K_{\text{dAC:Gs}}$	dissociation constant for G-protein with AC	0.2250	$\mu\text{M}$	Step 2 <sup>1</sup>

**Supplemental Table 1: Summary of model parameters in the receptor module.** Steps for parameter estimation are described above.

Explicit algebraic equations:

$$Ra = \frac{Ri}{K_R}$$

$$LRi = \frac{Ltot * Ri}{K_R}$$



$$LRa = \frac{Ltot * Ra}{\alpha_L * K_L}$$

$$RaG = \frac{Ra * G}{K_G}$$

$$LRaG = \frac{LRa * G}{\gamma_L * K_G}$$

$$ARi = \frac{Atot * Ri}{K_A}$$

$$ARa = \frac{Atot * Ra}{\alpha_A * K_A}$$

$$ARaG = \frac{ARa * G}{\gamma_A * K_G}$$

$$\beta 1ARact = \beta 1ARtot - \beta 1AR_{S464} - \beta 1AR_{S301}$$

$$G_{act} = kg_{act} * (RaG + LRaG + ARaG)$$

Implicit algebraic equations solved by differential-algebraic solver:

$$0 = \beta 1ARact - Ra - LRi - LRa - RaG - LRaG - ARi - ARaG - Ri$$

$$0 = G_{stot} - LRaG - RaG - ARaG - G$$

<b>Description</b>	<b>Calibration or Validation</b>
Figure 2A ligand binding EC <sub>50</sub>	Validation
Figure 2B cAMP kinetics	Validation
Figure 2C cAMP basal and max	Calibration of K <sub>G</sub> and γ <sub>L</sub>
Figure 2C cAMP EC <sub>50</sub>	Validation
Figure 2D PKA activity kinetics	Validation
Figure 2E PLB phosphorylation EC <sub>50</sub>	Validation
Figure 2F Ca <sup>2+</sup> EC <sub>50</sub>	Calibration of K <sub>L</sub> for ISO
Figure 3B-F Ca <sup>2+</sup> sensitivity to ISO+PRO	Validation
Figure 4B PKA sensitivity to ISO+PRO	Validation
Figure 6 Ca <sup>2+</sup> sensitivity to ISO+MET and ISO+CAR	Validation
Figure 7A,B ligand binding change in EC <sub>50</sub> and AC activity minimum for Arg389 receptor	Calibration of K <sub>G</sub> for Arg389 receptor
Supplemental Figure 2 cAMP synthesis for 19 ligands	Calibration of α
Supplemental Figure 4 PRO/MET/CAR dose responses + 0.1 μM ISO	Validation
Supplemental Figure 7 ISO+ 0.3 μM CAR	Validation

**Supplemental Table 2. Summary of model validations and calibrations.** The description indicates the specific features that can be compared between model and experiment.

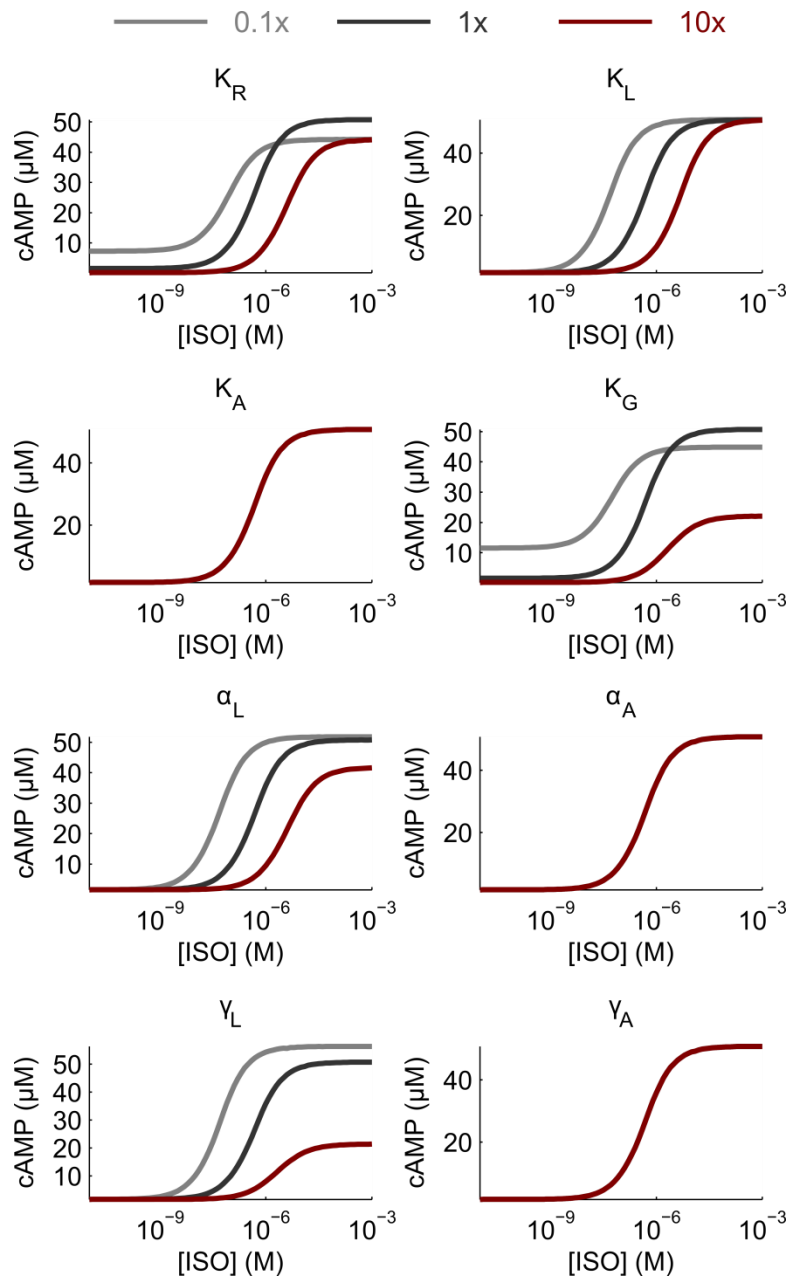
### *Alternative model for carvedilol binding to the β<sub>1</sub>-adrenergic receptor*

To reconcile the discrepancy between model and experiments with low dose 0.3 μM CAR (Supplemental Figure 6), the CAR model was updated based on studies by Kindermann et al.<sup>11</sup>. Kindermann et al. provided data to support that CAR persistently binds the β-adrenergic receptor after washout by binding to a second, allosteric site on the receptor. Based on this mechanism, we developed an alternate model to include CAR binding to the allosteric site by modifying G-protein activation:

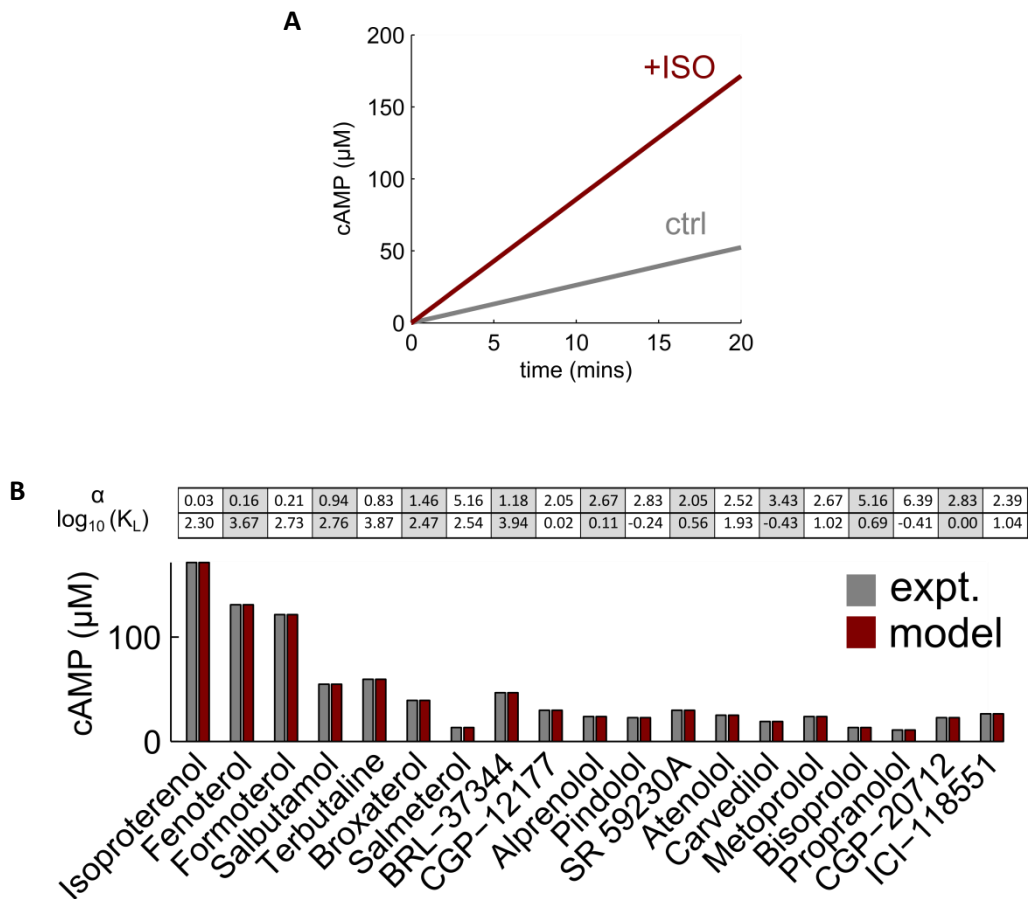
$$G_{act} = kg_{act} * (RaG + LRaG + ARaG) \frac{Kd_{CAR}}{Kd_{CAR} + [CAR]}$$

K<sub>d</sub><sub>CAR</sub> (binding affinity to the allosteric site) was assumed to be equal to K<sub>L</sub> (binding affinity to the orthosteric site) for CAR. The alternate model correctly predicts the lack of adrenergic responsiveness with 0.3 μM CAR (Supplemental Figure 7).

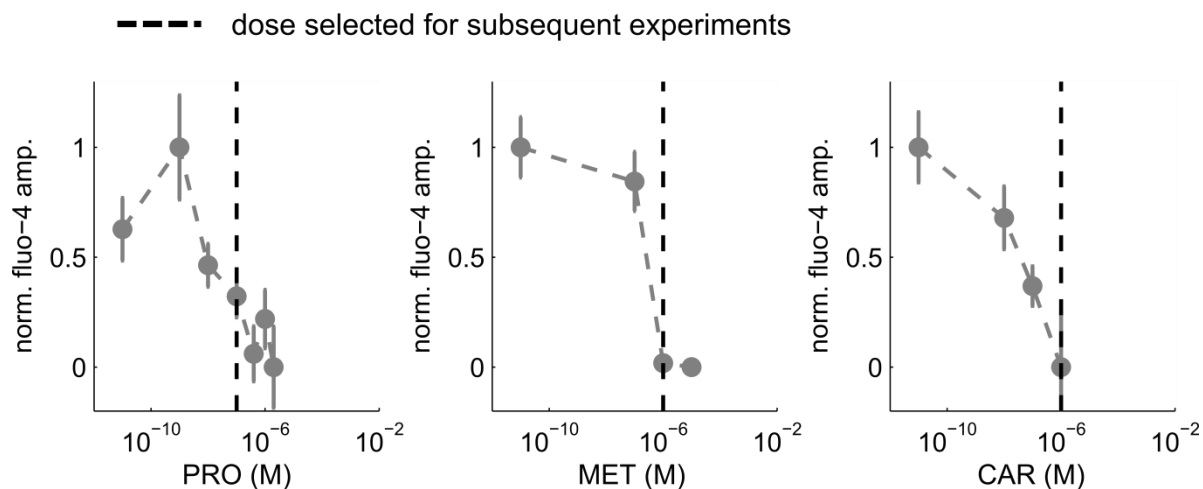
## Supplemental Figures



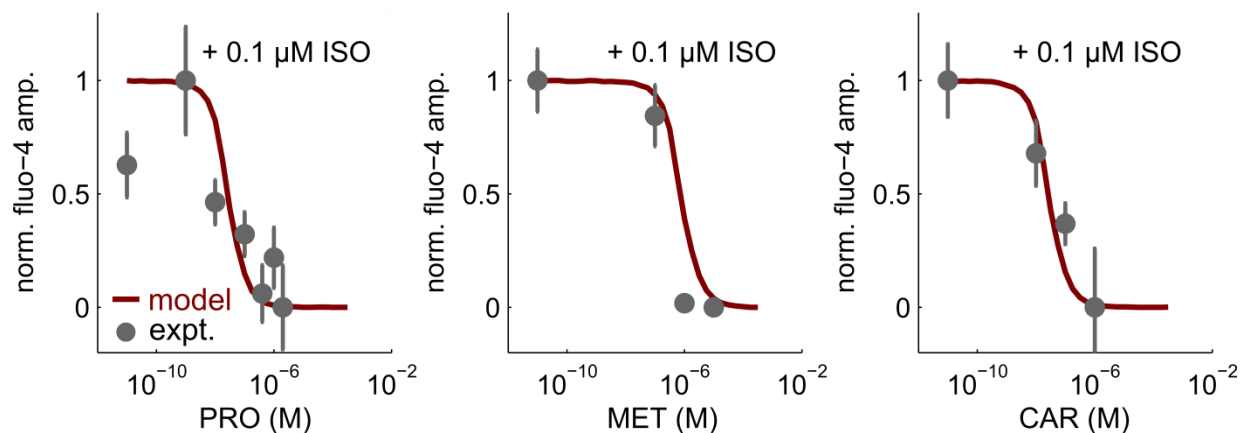
**Supplemental Figure 1: Sensitivity analysis of signaling module.** Each parameter of the ETCM was increased or decreased by 10-fold to determine the effect on downstream cAMP. This analysis revealed that  $K_R$  and  $K_G$  are the only parameters in the ETCM that affect basal cAMP, and both parameters have a biphasic effect on maximal cAMP.  $\gamma_L$  has a substantial role on maximal cAMP.  $K_L$  specifically affected the  $EC_{50}$ .  $K_A$ ,  $\alpha_A$  and  $\gamma_A$  did not have an effect in these simulations because no antagonist was applied.



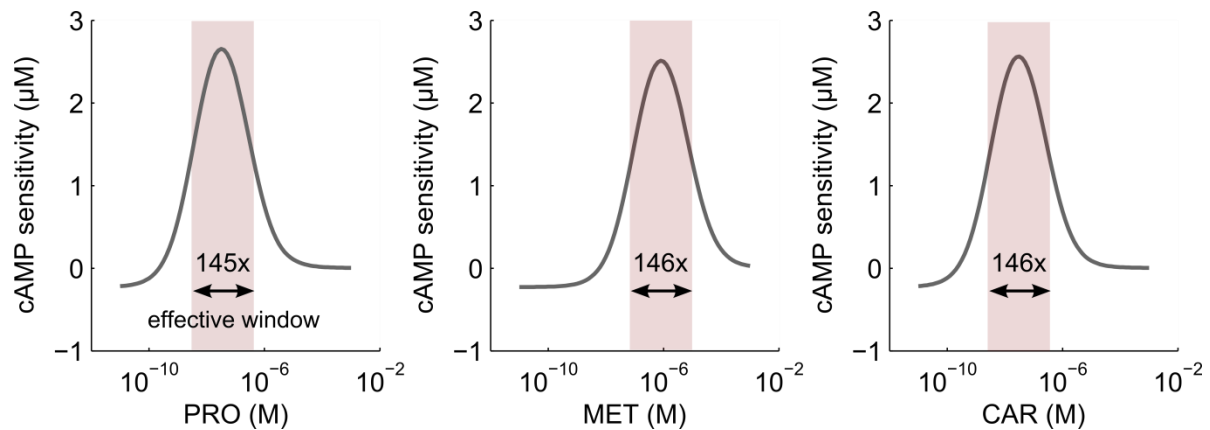
**Supplemental Figure 2: Estimation of ligand specific parameters  $\alpha$  and  $K_L$  for 19 ligands.** **A**, Range of cAMP synthesis rates in model under control and saturating isoproterenol concentration. **B**, The model was calibrated to cAMP synthesis rates for 19 ligands from Hoffmann et al. to estimate the inverse agonism parameter  $\alpha$ . The corresponding  $K_L$ , shown in units of  $\log_{10}(K_L \text{ nM})$ , was then calculated as described in Supplementary Methods.



**Supplemental Figure 3: Experimental dose response of  $\beta$ -blockers in isolated rat ventricular myocytes in the presence of 0.1  $\mu$ M ISO.** The vertical dashed line represents empirically determined doses for propranolol (0.1  $\mu$ M), carvedilol (1  $\mu$ M), and metoprolol (1  $\mu$ M), that were just sufficient to suppress  $\text{Ca}^{2+}$  transient response to 0.1  $\mu$ M isoproterenol. These doses were then selected for use in subsequent experiments shown in Figure 6. Plots are normalized between the  $\text{Ca}^{2+}$  transient amplitude of untreated myocytes and the maximum seen with 0.1  $\mu$ M ISO.

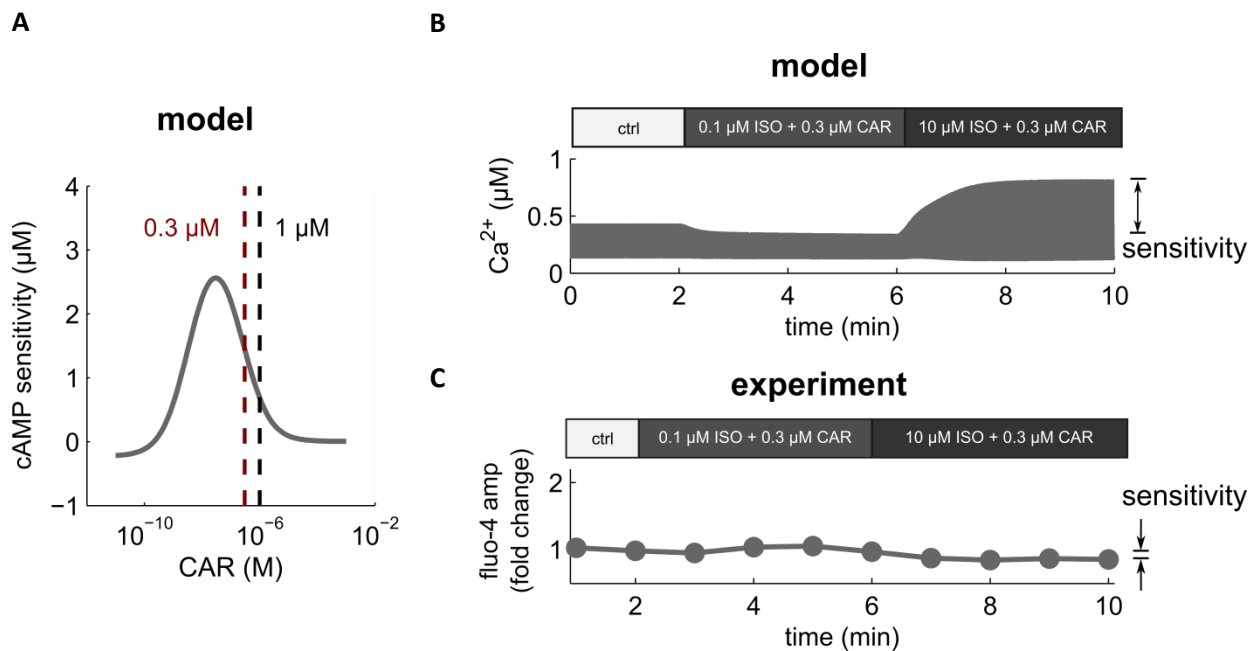


**Supplemental Figure 4: Model predicts  $\beta$ -blocker dose response in the presence of 0.1  $\mu$ M ISO.** This figure shows accurate validation of model predictions of  $\text{EC}_{50}$  for propranolol, metoprolol and carvedilol.

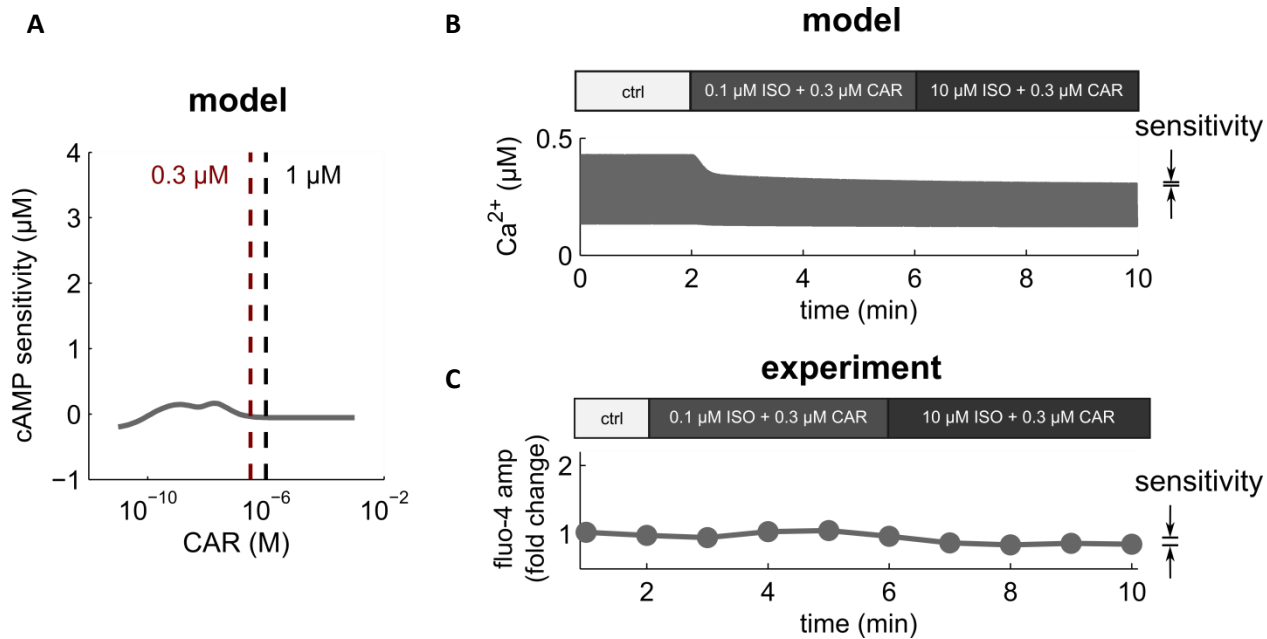


**Supplemental Figure 5: Computational dose response of cAMP sensitivity for 3  $\beta$ -blockers.**

Simulations were performed as in Figure 6, but for varying levels of propranolol, metoprolol or carvedilol. For all 3  $\beta$ -blockers, these simulations predicted an effective window of concentration that could maintain cAMP sensitivity. Effective window was quantified as the fold-change in concentration over which cAMP sensitivity was at least half-maximal for that ligand. Note that the doses used in Figure 6 (which were determined empirically in Supplemental Figure 3 and validated for the model in Supplemental Figure 4) are within the effective window for propranolol and metoprolol but outside the predicted effective window for carvedilol.

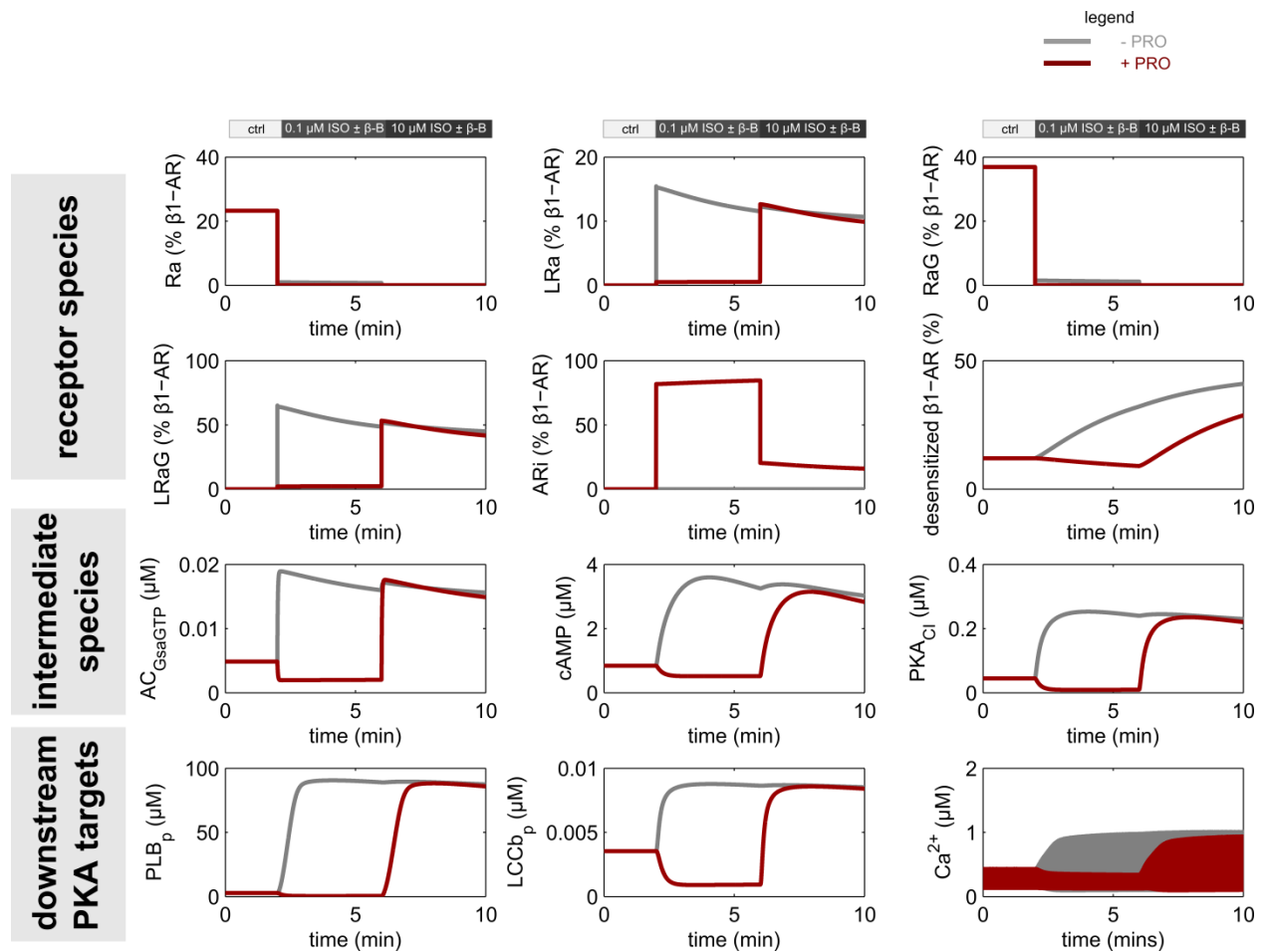


**Supplemental Figure 6: Model fails to predict the measured lack of  $\beta_1$ -adrenergic responsiveness in cells treated with 0.3  $\mu\text{M}$  CAR.** **A**, Computational dose-response of cAMP sensitivity for CAR. Red dashed line indicates new CAR dose used in experiments (0.3  $\mu\text{M}$ ). **B**, The model predicted that CAR inhibits response to 0.1  $\mu\text{M}$  ISO but maintains the 10  $\mu\text{M}$  ISO response (similar to propranolol and metoprolol). **C**, In disagreement with model predictions, isolated cardiac myocytes with 0.1  $\mu\text{M}$  ISO + 0.3  $\mu\text{M}$  CAR were not responsive to further stimulation with 10  $\mu\text{M}$  ISO.

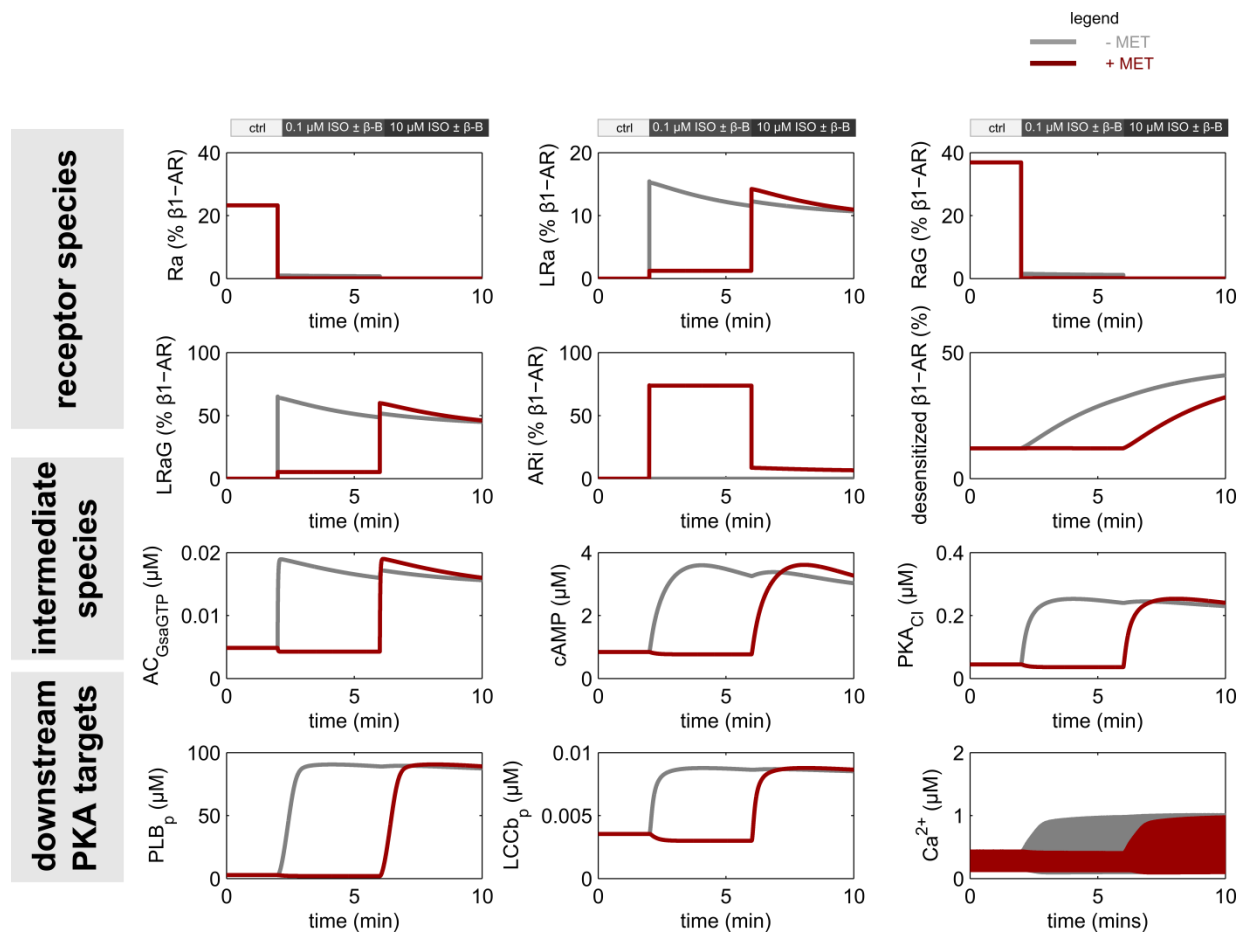


**Supplemental Figure 7: Alternate receptor model incorporating allosteric carvedilol binding accurately predicts reduced  $\beta_1$ -adrenergic responsiveness in cells treated with 0.3  $\mu\text{M}$  CAR.** In (A) and (B), the model predicts that  $\beta_1$ -adrenergic responsiveness to further stimulation with 10  $\mu\text{M}$  ISO is diminished, in agreement with experiments (C).

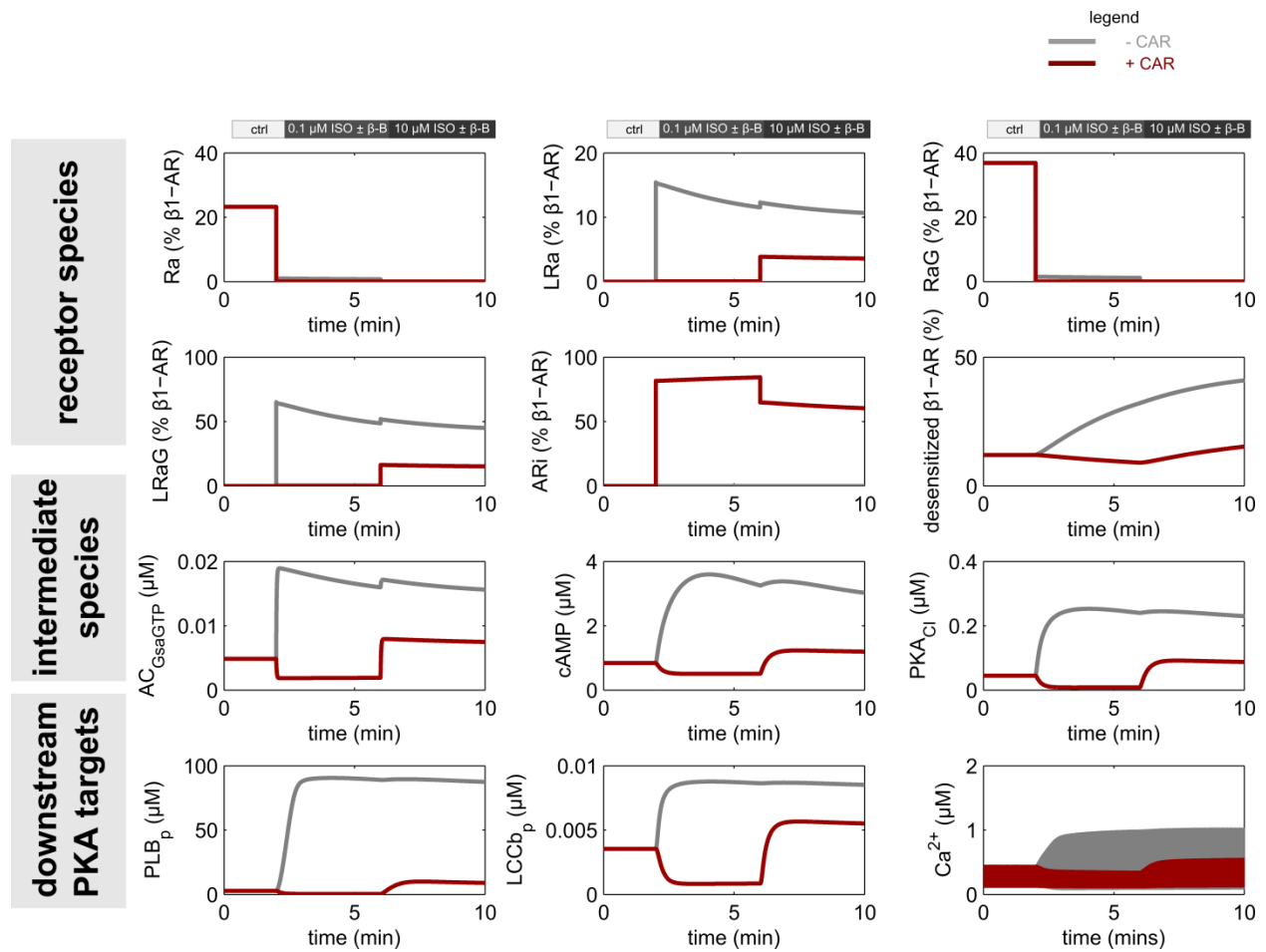




**Supplemental Figure 8: Predicted effect of propranolol on receptor states and downstream signaling components.** Note that with low ISO, propranolol is predicted to prevent  $\beta 1$ -AR desensitization and maintain receptors in inactive states (ARi). However with subsequent high ISO the propranolol is displaced, allowing downstream effects on cAMP/PKA/Ca<sup>2+</sup> but also receptor desensitization.



**Supplemental Figure 9: Predicted effect of metoprolol on receptor states and downstream signaling components.** Note that with low ISO, metoprolol is predicted to prevent  $\beta$ 1-AR desensitization and maintain receptors in inactive states (ARi). However with subsequent high ISO the metoprolol is displaced, allowing downstream effects on cAMP/PKA/Ca<sup>2+</sup> but also receptor desensitization.



**Supplemental Figure 10: Predicted effect of carvedilol on receptor states and downstream signaling components.** In contrast to propranolol and metoprolol, carvedilol is predicted to prevent  $\beta 1$ -AR desensitization and maintain receptors in inactive states (ARi) at both low and high ISO. Thus carvedilol prevents downstream effects on cAMP/PKA/Ca<sup>2+</sup> and receptor desensitization even at high ISO.

## References

1. Saucerman, J. J., Brunton, L. L., Michailova, A. P. & McCulloch, A. D. Modeling {beta}-Adrenergic Control of Cardiac Myocyte Contractility in Silico. *J Biol Chem* **278**, 47997–48003 (2003).
2. Saucerman, J. J. & McCulloch, A. D. Mechanistic systems models of cell signaling networks: a case study of myocyte adrenergic regulation. *Prog. Biophys. Mol. Bio.* **85**, 261-78 (2004).
3. De Lean, A., Stadel, J. M. & Lefkowitz, R. J. A ternary complex model explains the agonist-specific binding properties of the adenylate cyclase-coupled beta-adrenergic receptor. *J. Biol. Chem.* **255**, 7108–7117 (1980).
4. Samama, P., Cotecchia, S., Costa, T. & Lefkowitz, R. J. A mutation-induced activated state of the beta 2-adrenergic receptor. Extending the ternary complex model. *J. Biol. Chem.* **268**, 4625–4636 (1993).
5. Kjelsberg, M. A., Cotecchia, S., Ostrowski, J., Caron, M. G. & Lefkowitz, R. J. Constitutive activation of the alpha 1B-adrenergic receptor by all amino acid substitutions at a single site. Evidence for a region which constrains receptor activation. *J. Biol. Chem.* **267**, 1430–1433 (1992).
6. Rosenbaum, D. M. *et al.* Structure and function of an irreversible agonist-[bgr]2 adrenoceptor complex. *Nature* **469**, 236–240 (2011).
7. Engelhardt, S., Grimmer, Y., Fan, G. H. & Lohse, M. J. Constitutive activity of the human beta(1)-adrenergic receptor in beta(1)-receptor transgenic mice. *Mol. Pharmacol.* **60**, 712–717 (2001).
8. Ljung, L. *System Identification: Theory for the User.* (Pearson Education, 1998).
9. Vila Petroff, M. G., Egan, J. M., Wang, X. & Sollott, S. J. Glucagon-like peptide-1 increases cAMP but fails to augment contraction in adult rat cardiac myocytes. *Circ. Res.* **89**, 445–452 (2001).
10. Hoffmann, C., Leitz, M. R., Oberdorf-Maass, S., Lohse, M. J. & Klotz, K.-N. Comparative pharmacology of human beta-adrenergic receptor subtypes--characterization of stably transfected receptors in CHO cells. *Naunyn. Schmiedebergs Arch. Pharmacol.* **369**, 151–9 (2004).
11. Kindermann, M. *et al.* Carvedilol but not metoprolol reduces beta-adrenergic responsiveness after complete elimination from plasma in vivo. *Circulation* **109**, 3182–3190 (2004).